SEBS colonized in ileal mucosa, optimized bacterial composition, improved Se level and activated TLR2 NF-kB1 signaling pathway to regulate β-defensin 1 expression

Jiajun Yang
College of Veterinary Science
Jing Wang
College of Veterinary Science
Minhong Zhang
Institute of Animal Science
Dong Wu
The institute of Animal Husbandry and Veterinary Medicine
Kai Zhan
The institute of Animal Husbandry and Veterinary Medicine
Chonglong Wang
The Institute of Animal Husbandry and Veterinary Medicine
Yijing Wu
The institute of Animal Husbandry and Veterinary Medicine
Pengcheng Yu
National Institute for Viral Disease Control and Prevention
Zongliang Liu
Hefei Zhien Biotechnology Company Limited
Kehe Huang (khhuang@njau.edu.cn)
College of Veterinary Science https://orcid.org/0000-0003-3844-0055
Zhanyong Wei
The College of Animal Science and Veterinary Medicine

Research

Keywords: Selenium, bacillus subtilis, BD1, inflammation, immune system, GIT, probiotic bacteria

Posted Date: July 2nd, 2020

DOI: https://doi.org/10.21203/rs.3.rs-38246/v1

Abstract

Background

Both selenium (Se) and probiotic *bacillus* improve immunity. Beta defensin 1 (BD1), a component of intestinal mucosal immunity, could be up-regulated in dietary selenium enriched *bacillus subtilis* (SEBS) supplementation. SEBS was supplemented in the culture medium of mouse intestinal crypt cells and the diets of chicks to observe the effects of SEBS on BD1 in the intestine by colonization of *bacillus subtilis*, its recognition and signaling pathway, bacterial composition optimization, and biological functions of Se.

Results

BD1 was formed in intestinal crypt cells and secreted into the lumen through the villi brush border. BD1 was up-regulated in distal ileum segments with SEBS and *bacillus subtilis* colonization. This occurred through the recognition of toll like receptor 2 and the NF-kB1 signaling pathway (TLR2-MyD88NF-kB1), this increased expression was further enhanced with Se combination. Pro-inflammatory cytokines, TNF-α, IL-1β, and IL-6, were up-regulated with *bacillus subtilis* supplementation, while this up-regulation was inhibited with Se. Colonization of *bacillus subtilis* in distal segments of the ileum improved bacterial diversity, while reducing the number of endogenous *Salmonella* and *lactobacilli sp*. in ileal mucous membranes with SEBS supplementation. Species of unclassified *Lachnospiraceae*, uncultured *Anaerosporobacter*, *Ruminococcaceae_UCG-014*, *Peptococcus*, and *Lactobacillus salivarius*, and unclassified *Butyricicoccus* were substantial in ileal mucous membranes to promote BD1 concentration.

Conclusion

SECB, colonized in the ileal mucous membrane, optimized bacterial composition, enhanced BD1 secretion through activation of the TLR2-MyD88NF-kB1 signaling pathway, and reduced pro-inflammatory factors. Our results suggest a new avenue for the combination of probiotic bacteria and essential micro-element selenium to improve intestinal mucosal immunity, increase defense against cold stress, and reduce illness incidence and mortality.

Background

The low temperature of living condition easily causes to cold stress to animals, led to weak immunity. Hence, improve body immunity is crucial to prevent the pathogenic infection. Probiotics contain live microorganisms and spores and confer health benefits to the host when administered in adequate amounts [1]. Certain strains of *bacillus subtilis* (*B. subtilis*) are used as probiotic bacteria, contributing a myriad of benefits to immunity and metabolism [2]. Certain probiotic *B. subtilis* was administrated orally, survived and colonized in intestinal mucous membrane, optimized the composition of microbiota, which were positively stimulating the intestinal immunity and metabolism. These benefits assist in overcoming

infection stress and clearing pathogens [3]. The relationship between intestinal innate immunity and bacterial composition is close and direct. Beta defensins of the innate immune system have been found in species of bird, human, several domestic animals, and mice [4, 5]. Beta defensin 1 (BD1) is expressed and distributed in several organs, such as the intestine, lungs, and bone marrow [6, 7]. In the gut, BD1 is formed and secreted by intestinal epithelial cells [8]. BD1 was shown to be involved in the induction of other beta defensins, such as BD2, BD3, and BD4 [9]. The antibacterial ability of BD1 is the strongest among all β-defensins and plays a pivotal role in mucosal immunity, specifically protecting against infection in the gut [10–12].

Probiotic *B. subtilis* colonized in mucous membranes strengthen the probiotic effect and produce microbial-associated molecular patterns (MAMPs), which could be recognized by toll-like receptors (TLRs) [13], resulting in a signal cascade to mobilize and activate the innate immune system [2]. TLRs are a series of membrane receptors that detect extra-cellular microbes and trigger signaling cascades for their eradication [14, 15]. Leukocyte pro-inflammatory cytokines, such as IL-1β, IL-6, and TNF-α, are known as potent inducers and up-regulators of defensins [16, 17]. They activate the NF-kB pathway, causing NF-kB entry to the nucleus, inducing the production of inflammatory cytokines, and provoking the rapid activation of innate and adaptive immune system factors, such as BD1. *Bacillus* was composed mainly by peptidoglycan and proteide, the core was spore [18]. However, there is still unknown that probiotic *bacillus* as a whole recognized by which TLRs.

Selenium (Se) is an important trace element and its beneficial effects are well documented [19]. Suitable doses of Se supplementation can regulate metabolism and antioxidation, especially during bodily stress and Se deficit areas [20]. Since Se confers several benefits, it is urgent to explore a cheap and convenient organic Se source for supplementation. Meanwhile, Se can help the immune cells to defense the infection caused by pathogen. Still the supplementation of Se could reduce the DNA copy number of pathogens to inhibit pathogenic infectious effects, alleviate the infected cell numbers and stress response [21, 22].

Considering the beneficial effects of Se and *B. subtilis* on immunity and stress [23], it would be valuable to study Se and *B. subtilis* in combination to determine whether greater effects are induced when administered together. To test this hypothesis, and observe the potential mechanism, we produced Se-enriched *B. subtilis* (SEBS), which combines the virtues of *B. subtilis* and those of organic Se. The intestinal crypt cells of mice were cultured and treated with SEBS to explore the effects and signaling pathways associated with BD1. Chinese Huainan Partridge chicken is a dual-purpose native breed from South China [2], which was used in our study to observe the regulation of BD1 mechanisms by SEBS *in vivo* in cold condition (Fig. 1). This study first discovered that the bacteria of *B. subtilis* colonized in ileal mucous membrane was recognized by the TLR2 and presentation to MyD88, stimulating and provoking downstream signals of IRAK, TRAF6, IκB, IL-1β, and TNF-α. The signaling pathway is the classic TLR2-MyD88-NF-kB1 pathway. Meanwhile, the inflammatory response of intestinal crypt cells provoking by *B. subtilis* could be alleviated under the action of Se, while the whole immune status of intestine was still improved with combined use of Se and *B. subtilis*. The colonization of *B. subtilis* in ileal mucous membrane optimized the intestinal bacterial composition, which improved the anti-infection ability. This

study could provide novel insights regarding combined use of probiotic bacteria and essential micro-element Se.

Methods

Preparation and analyses of SEBS

B. subtilis was isolated from the ileum of a healthy Chinese Huainan Partridge chicken by our research group, the institute of animal husbandry and veterinary medicine, Anhui Academy of Agricultural Sciences, and stored in the China General Microbiological Culture Collection Center (CGMCC), the strain number is CGMCC 14246. The 16S ribosomal DNA was sequenced and deposited at the National Center for Biotechnology Information (NCBI) of the United States of America (USA), the access number is KT260179. We cultured *B. subtilis* using a liquid beef extract–peptone medium. The fermentation of selenium-enriched *B. subtilis* was prepared with sodium selenite supplemented into the culture medium. The morphologic and structural properties of bacteria between *B. subtilis* and SEBS was monitored using a scanning electron microscope (SEM) and transmission electron microscopy (TEM). The bacteria of *B. subtilis* and SEBS was concentrated via centrifugation at 3, 000 rpm, and immersed in a 5% glutaraldehyde solution for 24 h [24]. Se concentration in the supernatant and precipitate of *B. subtilis* and SEBS fermented medium was calculated using atomic absorption spectrometry and the live bacteria was enumerated with yeast extract peptone dextrose medium after term serial dilution.

Animal Studies

Chicks and management

For the chicken origin of *B. subtilis* and SEBS, homologous feeding of probiotic bacteria could play more beneficial roles than non-homologous. The strain of *B. subtilis* was isolated from Chinese Huainan Partridge chicken. Hence, Chinese Huainan Partridge chickens were chosen to carry out the animal study. Animal experiments were approved and performed in accordance with the experimental guidelines of the Institutional Animal Care and Use Committee of China. The experimental protocols in this study, including animal husbandry and slaughter, were approved by the Institute of Animal Science and Welfare of Anhui Province (no. IASWAP2017120649). A total of 500 one-d-old Chinese Huainan Partridge chickens (average body weight, 40.15 g) were randomly allocated to five groups with five replicates of 20 each. For the duration of the starter diet, the pen space for each replicate was 2.3 m^2. The room temperature was maintained at 33–35 ℃ using an electric heating tube in the first week, then gradually declined to 21 ℃ at the end of the fourth week. At the end of the starter diet period, all chicks were weighed and transferred into larger pens (5.6 m^2 for each replicate); chicks in the previous replicate were also transferred and housed under the same conditions. In the fifth week, the temperature was maintained at 18–20 ℃ using infrared warming lights. In weeks six to eight, the number of infrared warming lights was reduced gradually for a room temperature of 6.5 ℃. The chickens were allowed *ad libitum* access to water and

feed throughout the experimental period. The normal immune procedure was implemented throughout the trial.

Feed for each group

Chickens in the control group were fed a basal diet and the four treatment groups were fed the following: basal diet with either inorganic sodium selenite (IS), *B. subtilis* (BS), selenium enriched *B. subtilis* (SEBS), and flavomycin. Experimental diets were fed in two periods: starter (days 0–28) and finisher (days 29–56). The basal diet composition and nutrient analysis results, which did not contain any probiotics or antibiotics, are shown in Supplementary Table 1 (Table S1). All nutrients met or exceeded the nutrient requirements (National Research Council, 2012) [25]. Diet for chickens in the IS group, 1.12 g of sodium selenite (analytically pure) was diluted into 100 mL distilled water, which was blended with 5 kg of feed. Thereafter, the mixed mass feed was added to a blender containing 90 kg of mass feed. The blender was employed for 20 min to ensure uniform mixing of additives. The feed for the flavomycin group was prepared using 4 g premixed food containing 10% flavomycin, which was blended with 100 kg of feed, to reach a concentration of 4 mg/kg. For *bacillus*, 50 mL *B. subtilis* fermentation liquid was measured separately and first blended with 5 kg of feed, and then with 95 kg of mass feed. The SEBS feed was prepared by blending 1000 mL of SEBS fermentation liquid with 100 kg of feed. After preparing the five different feedstuffs, the population of *B. subtilis* was counted using the plate method with a yeast extract peptone dextrose medium. The concentration of Se in all feed types was also measured. The results are listed in Table S2.

Performance and sample collection

Chicks in every replicate of each treatment group were weighed on 0 d and 56 d. Daily feed consumption was accurately recorded. After 56 d, 2 average body weight of chickens in each replicate were selected (n = 5×2), fasted for 12 h, and then the tissue and blood were harvested under general halothane anesthesia. All blood samples were collected in 5.0 mL sterile heparinized tubes. Blood was centrifuged at 3000 rpm for 10 min to collect the plasma for biochemical assays. Blood samples (1 mL) was removed to measure the Se concentration. Tissues of the jejunum and ileum were removed under aseptic conditions, stored in sterile plastic tubes in boxes packed with ice, and immediately transported to our laboratory for quantification of bacteria and other assays.

FISH assay

Two strains of bacteria, *B. subtilis* and endogenous *salmonella* [26], residing in the GIT were investigated using fluorescence *in situ* hybridization (FISH). Ileal mucosal samples (0.3 g) were fixed by immersion in 10% formaldehyde for 24 h. A 50 μL volume of homogeneous tissue liquid was transferred to poly-L-lysine-coated slides, which were then air dried on a sterile benchtop for 3 h. The tissue was incubated with lysozyme at 32 ℃ for 10 min; the slide was then washed with distilled water and immersed in 70% ethanol for 2 min, followed by air drying. Probes with carboxytetramethylrhodamine and 6-carboxy-fluorescein were designed and conjugated with *B. subtilis* and *salmonella*, respectively. The length of the *B. subtilis* genetic probe was long to ensure specific integration with samples. Probe sequences of *B.*

subtilis and *salmonella* are listed in Table S3. Probes were diluted to 60 nM, denatured at 95 ℃ for 5 min, and maintained at 4 ℃ before use. A probe (12 μL) was added to the tissue, followed by incubation at 46 ℃ for 12 h, and washed with phosphate buffer solution (pH 7.4). The tissue was stained with 4',6-diamidino-2-phenylindole for 5 min, then washed three times with distilled water for 5 min each. After drying, the slides were mounted with fluoromount-GTM (Abcam, Cambridge, UK) and observed with a fluorescence microscope (BX53; Olympus, Tokyo, Japan).

qRT-PCR for number of B.subtilis

After fermentation in beef extract–peptone medium, a tenfold dilution series of *B. subtilis* KT260179 was planned. Colonies of *B. subtilis* were counted using the plate method under a microscope to obtain samples of 1×10^4, 10^5, and 10^6. Total RNA in each dilution was extracted using the RNA Extraction Kit (Invitrogen, Carlsbad, CA, USA). Reverse transcription was performed using a GoScript Reverse System (Invitrogen). First-strand cDNA was synthesized by incubating a reaction mixture containing 11 μL RNA and 1 μL RNase-free dH_2O at 70 ℃ for 3 min, followed by 0 ℃ for 5 min. A dNTP mixture (1 μL; 10 mmol/L), 4 μL GoScript 5X reaction buffer, 1 μL GoScript reverse transcriptase, 1.5 μL Mg^{2+} (25 mM), and 0.5 μL RNase inhibitor were combined in a total volume of 20 μL and incubated at a 37 ℃ in a water bath. Primers were designed according to the 16S rRNA of *B. subtilis* KT260179, which are described in Table S4. Amplification was performed in a 20 μL mixture containing 10 μL of 2 × qPCR SYBR Premix Ex-Taq, 2 μL template cDNA, 0.5 μL each primer (10 μmol/L), and 7 μL PCR-grade water. The cycling protocol was as follows: 95 ℃ for 30 s, followed by 40 cycles of 95 ℃ for 5 s and 60 ℃ for 30 s, and one cycle for melting curve analysis, consisting of 95 ℃ for 60 s, 65 ℃ for 60 s, and 95 ℃ for 1 s. The amplification curve was generated based on the dilution of the standard curve of *B. subtilis* KT260179. The standard curve of *B. subtilis* KT260179 was described according to the results of quantitative real-time polymerase chain reaction (qRT-PCR).

Samples (0.2 g) of mucous membrane from the distal segment of the ileum were prepared to extract total RNA and qRT-PCR was carried out as described above to evaluate colonization of *B. subtilis*.

Plate method

The distal segment ileum samples were cut open and washed with sterilized physiological saline (pH 7.0). Samples of ileal mucous membrane were scratched from the ileum using a slide. The ileal mucous membrane and cecal lumen contents (0.4 g each) were prepared and 10-fold dilutions were prepared with sterilized saline. The bacterial composition of the ileal mucous membrane and cecal lumen contents in all groups was determined using the plate method. Salmonella Shigella agar was used for *salmonella* and MRS agar was used for lactic acid bacteria [3, 27]. The assays were repeated three times. After the cecal content dilution had been heated (80 ℃) for 15 min to inactivate bacteria, *bacillus* remained. The total number of *bacillus* was counted using beef extract peptone medium. *Salmonella* and *bacillus* were cultured at 37 ℃ aerobic conditions, total lactic acid bacteria were cultured under anaerobic conditions.

Gut bacterial 16 s rDNA sequence and analysis

Samples (0.25 g) of the ileal mucous membrane were prepared (n = 50). Microbial DNA was extracted from these samples using the E.Z.N.A.® soil DNA Kit (Omega Bio-tek, Norcross, GA, USA) according to the manufacturer's protocol. The final DNA concentration and purification were determined using a NanoDrop 2000 UV-vis spectrophotometer (Thermo Scientific, Waltham, MA, USA), and DNA quality was determined using 1% agarose gel electrophoresis. The V3-V4 hypervariable regions of the bacteria 16S rRNA gene were amplified with primers *338F* (5'-ACTCCTACGGGAGGCAGCAG-3') and *806R* (5'-GGACTACHVGGGTWTCTAAT-3') using a thermocycler PCR system (GeneAmp 9700, Applied biosystems, Foster City, CA, USA). PCR was conducted as follows: 3 min denaturation at 95 ℃, 27 cycles: 30 s at 95 ℃, 30 s annealing at 55 ℃, 45 s elongation at 72 ℃, and a final extension at 72 ℃ for 10 min. PCR was performed in triplicate 20 μL mixtures containing 4 μL of 5 × FastPfu Buffer, 2 μL of 2.5 mM dNTPs, 0.8 μL of each primer (5 μM), 0.4 μL of FastPfu polymerase, and 10 ng of template DNA. The resulting PCR products were extracted from a 2% agarose gel and further purified using the AxyPrep DNA Gel Extraction Kit (Axygen Biosciences, Union City, CA, USA) and quantified using QuantiFluor™-ST (Promega, Madison, WI, USA) according to the manufacturer's protocol. Purified amplicons were pooled in equimolar and paired-end sequenced (2 × 300) on an Illumina MiSeq platform (Illumina, San Diego, CA, USA) according to standard protocols. The Illumina sequencing raw data has been deposited into Sequence Read Archive database (SRP) of The National Center for Biotechnology Information (NCBI) of The United States of America (SRR10948561). The BioProject accession is PRJNA602383.

Diversity metrics were calculated using the core-diversity plugin within QIIME2. Feature level alpha diversity indices and operational taxonomic units (OTUs) were used to estimate the microbial diversity within an individual sample. Beta diversity distance measurements were performed with weighted UniFrac to investigate the structural variation in the microbial communities across samples, and then visualized via principal coordinate analysis (PCoA). Co-occurrence analysis was performed by calculating Spearman's rank correlations between predominant bacterial species and the network plot. Additionally, the potential KEGG Ortholog (KO) functional profiles of microbial communities were predicted using PICRUSt.

Immunohistochemical assay

Intestinal sections, 2 mm in length from ileum of chick, were collected and immediately placed in 10% buffered formalin overnight at room temperature. Paraffin-embedded tissues were cut into 4 μm slices. The slides containing paraffin-embedded ileum were first deparaffinized using 100% xylene and rehydrated by decreasing ethanol percentages. Subsequently, the slides were then incubated in a bath (containing 10 mmol/L sodium citrate) at 90 ℃ for 60 min for antigen retrieval and were next transferred to a bath of 0.20% sodium borohydride to block the endogenous peroxides. After washing three times with PBS, the slides were blocked in blocking buffer containing 0.025% Triton X-100, 2% FBS, and 5% BSA at 25 ℃ for 60 min. Slides were further incubated in monoclonal-proliferating cell nuclear antigen antibody (1:500 dilution; BIOSS, Beijing, China) overnight at 4 ℃ in a humidified chamber. Slides were then incubated with the biotin-conjugated goat anti-chick immunoglobulins (1:250 dilution; BIOSS) at 25 ℃ for 90 min after the primary antibody was rinsed off. Thereafter, the slides were further treated with

1 mL of 3,3-diaminobenzidine tetrahydrochloride (ComWin Biotech, Beijing, China) to visualize the antigenic structures. Finally, slides were examined by an observer blinded to the treatment group. Computerized densitometric analyses of BD1 tissue expression in the images were performed using Image-Pro Plus version 5.0 software (Media Cybernetics Inc., Bethesda, MD, USA). Micro histological structures of intestines were visualized under a light microscope, and villous length and crypt depth of each crypt and villous of the tissue were enumerated using AxioVision version 4.6 software.

Elisa assay for BD1 level and activity of GPX

Samples of ileal mucous membrane (n = 10) were prepared with homogenization and ten times dilution. The ileal mucous membrane samples were investigated for types of glutathione peroxidase (GPX), namely cytoplasmic (GPX1) and gastrointestinal (GPX4), and BD1 [28]. Whole blood samples from chicks (1 mL) were harvested for plasma GPX (GPX2) measurement. This experiment was performed using an ELISA kit (Invitrogen).

The Se concentration assay

A ZEEnit 700 P atomic absorption spectrometer (Analytik Jena, Germany) was employed to determine the selenium levels in samples of whole blood, heart, and liver. All measurements were performed using hydride generation atomic absorption spectrometry (HG-AAS) [28]. Samples of whole blood (1 mL), liver (0.3 g) of chicks, and the supernatant and precipitate of fermented medium (3 mL) of *B. subtilis* and SEBS were placed in beakers and digested by adding 10 mL of a nitric acid–perchloric acid (HNO_3–$HClO_4$) mixture. The cooled mixture was made up to 10 mL with 5% hydrochloric acid solution. Eight replicates were used for each group.

Cell Studies

Preparation of mouse primary intestinal crypt cells

Mice are frequently used as an animal model to study mechanisms of substances, such as microorganisms and drugs. Mouse crypt cells, other than chicken, were prepared to unveil the target molecular signal (TLRs-NF-kB-BD1) via SEBS supplementation *in vivo*, which was more suitably adapted to other animals in clinical applications.

C57BL/6 mice (4 weeks old, specific-pathogen-free) were purchased from Anhui Provincial Hospital Experimental Teaching Center. The mice were sacrificed to obtain the ileum and placed into a sterilized glass plate (9 cm diameter) containing PBS (0 ℃). Fat and connective tissue were removed from the ileum. The intestine was opened longitudinally, and contents were washed with PBS. This process was repeated until the supernatant appeared clear. The ileum was cut, washed with PBS twice, and the supernatant was removed. Small pieces of intestine were shaking incubated with 100 U/mL collagenase (Sigma, USA) buffer (20 μg/mL neutral protease □, 32 mM HEPES, 127.5 mM NaCl, 3.15 mM KCl, 0.7 mM Na_2HPO_4, and 3 mM $CaCl_2$, pH 7.60, 37 ℃) for 90 min. The cell suspension was filtered through mesh

(grid size about 150 and 75 μm) and further diluted with serum-free medium. After sedimentation for 10 min at 4 ℃, the supernatant was discarded. The ileal crypt cells were centrifuged (3, 000 rpm), then re-suspended, and washed twice with the same serum-free medium at 4 ℃. Lastly, the crypt cells were re-suspended in DMEM/Ham F12 medium (Sigma, USA), containing 2% fetal bovine serum (FBS), 24 mM $NaHCO_3$, 2 mM L-glutamine, 0.2% (w/v) BSA, 100 nM dexamethasone, 5 mg/l transferrin, 0.8 μmol/L insulin, and antibiotics (100 IU/mL penicillin, 100 μg/mL streptomycin). The average viability of isolated crypt cells was stained with 0.4% trypan blue dye and reached 90.05% (n = 3). The average cell yield from each ileum preparation was 7.29×10^7 crypt cells (n = 3).

Mouse primary intestinal crypt cell cultures and treatments

Mouse crypt cells were cultured at 37 ℃, with 5% CO_2 in a humidified atmosphere. After 4 h culture duration, cell monolayers were washed twice with Hanks' balanced salt solution, and 10 mL of fresh DMEM/Ham F12 medium, containing 10% FBS, was added to the culture flask. After 48 h cultivation, the culture medium was removed, and the cell monolayers were digested with 1 mL pancreatin (work concentration 0.25%). Firstly, the cells were grown in 2 mL of fresh serum-free DMEM/Ham F12 medium for 45 h, and treated with PBS (control), or 0.125 μg/mL of Se (Na_2SeO_3, Sigma), *B. subtilis* (live bacteria 5.0×10^6 colony forming units per mL, CFU/mL), SEBS (live bacteria 5.0×10^6 CFU/mL, Se concentration 0.125 μg/mL), or 0.125 μg/mL of Se (Na_2SeO_3, Sigma) and *B. subtilis* (Se-BS) for 3 h. Secondly, the cells were cultured in 2 mL of fresh medium for 42 h, treated with agonists TLR2 (Pam3 Cys-Ser-Lys, Abcam), TLR4 (LPS E. coli O55:B5, Sigma-Aldrich, USA), and TLR6 (FSL-1, Sigma-Aldrich, USA), respectively, for 3 h [30]. After treatment with agonists, cells were inoculated with PBS, Na_2SeO_3, *B. subtilis*, SEBS, or Se-BS for 3 h, which agrees with the first step. Thirdly, the cells were cultured in 2 mL of fresh medium for 42 h, treated with anti-TLR2 protein (Abcam, Britain) for 3 h. Then, cells were inoculated with PBS, Na_2SeO_3, *B. subtilis*, SEBS, or Se-BS for 3 h, which agrees with the first step.

Thereafter, all cells from different groups in step one and two were collected for RNA extraction. Cytokines of *MyD88, IRAK, TRAF6, IκB, BD1, IL-1β*, and TNF-α were measured using qRT-PCR.

qRT-PCR for cytokine expression

Quantitative real-time PCRs were carried out using SuperReal PreMix Plus (SYBR Green, FP205) on an ABI 7900HT Fast Real-time PCR System. Relative expression levels of target genes were quantitatively normalized against the expression of *GAPDH* using the ΔΔCT method. First-strand cDNA was synthesized by incubating a reaction mixture containing 11 μL RNA and 1 μL RNase-free dH_2O at 70 ℃ for 3 min, followed by 0 ℃ for 5 min. The cDNAs were also used for PCR, and the PCR products were detected on 2% agarose gel. A dNTP mixture (1 μL; 10 mmol/l), 4 μL GoScript 5X reaction buffer, 1 μL GoScript reverse transcriptase, 1.5 μL Mg^{2+} (25 mM), and 0.5 μL RNase inhibitor were combined in a total volume of 20 μL and incubated at a 37 ℃ in a water bath. Primers for *MyD88, IRAK, TRAF6, IκB, BD1, IL-1β*, and *TNF-α* were designed according to the mouse RNA genes submitted to NCBI. All PCR primers used in this study are described in Table S4.

Chicken intestinal mucosa cell collection and qRT-PCR

Chicken mucosal tissues, collected from the distal segment of the ileum, were washed with ice-cold PBS to remove intestinal contents, and longitudinally cut into small specimens. Crypt cells were isolated using a PBS buffer containing 1 mM EDTA, 1 mM dithiothreitol, and 5% fetal bovine serum, with shaking at 37 ℃ for 10 min. This supernatant was filtered and combined with RPMI 1640 and centrifuged at 1,500 rpm to isolate crypt cells.

Samples of crypt cells were prepared to extract total RNA to evaluate the level of the target TLRs-BD1 post-SEBS supplementation *in vivo*. Relative expression levels of target genes were quantitatively normalized against the expression of *GAPDH* using the ΔΔCT method. Primers for *TLR2, IL-1β, IL-6, TNF-a*, nuclear factor kappa B1 (*NF-kB1*), *BD1*, and *IFN-γ* were designed according to the chicken RNA genes submitted to NCBI. All PCR primers used in this study are described in Table S4.

Statistical analyses

Body weight, Se concentration, qRT-PCR, western blotting and DNA sequencing data were subjected to one-way ANOVA using the GLM procedure of SPSS, with significance reported at $P < 0.05$. Means were further separated using Duncan's multiple range test. All data were statistically processed as repeated measures to determine interaction of Se and *B. subtilis*. A *P*-value of less than 0.05 was considered statistically significant.

Results

Analysis of SEBS

SEBS were harvested after fermentation of *B. subtilis* in medium containing sodium selenite. The medium appeared pale pink in color. The concentration of ionic Se in fermentation supernatant and precipitate of SEBS was measured using HG-AAS, and concentrations reached 1.77 μg/mL and 48.13 μg/mL, respectively. In precipitate, Se existed primarily as Se protein (valence 2-) and nano particles Se (valence 0) in the cell of *B. subtilis*. The live cell of *B. subtilis* and SEBS both reached $9.2 \cdot 10^8$ CFU/mL. The appearance and internal structure did not vary between *B. subtilis* and SEBS, this was proved using SEM and TEM (Fig. 2a, 2b).

Impact on growth performance and mortality

To compare the probiotic effect of *B. subtilis* and SEBS, the measurements regarding body weight of chicks and the results of growth performance and mortality of Chinese Huainan Partridge chickens are shown in Fig. 3. The final body weight of chicks with SEBS supplementation was significantly increased ($P < 0.01$) compared to those of the control and inorganic Se supplemented groups, indicating a body weight increase of 220 g (Fig. 3a). In suitable living temperature and nutrition, morbidity of chicks was not found in 0–5 weeks. Between 6–8 weeks for the cold condition, died chicks could be found. The mortality of chicks with *B. subtilis*, SEBS, and flavomycin supplementation was significantly reduced

(Fig. 3b, P < 0.01). The result with SEBS exposure appears lowest, with a decrease of 6.1 compared to controls (*P* < 0.01).

Colonization and levels of B. subtilis and SEBS in intestine

To explore the colonization of *B. subtilis* in intestinal mucous membranes, we designed an *in vivo* study and employed FISH and qRT-PCR. *B. subtilis* is indicated by green spots detected in the distal segment of the ileum, indicated by the FISH assay (Fig. 4a), with both *B. subtilis* and SEBS supplementation. The qRT-PCR assays agree with the FISH results. The standard curve of *B. subtilis* is based on the tenfold dilution series of fermented culture (Fig. 5b). *B. subtilis* growth increased while being monitored in the distal segment of the ileum (Fig. 4c, P < 0.01). However, *salmonella* decreased with *B. subtilis* and flavomycin supplementation (Fig. 4d). In contrast, *B. subtilis* supplementation increases the number of total lactic acid bacteria and bacillus in ileal mucous membranes (Fig. 4e).

SEBS optimized ileal microbiota

High-throughput sequencing of all samples produced a total of 602,704 clean tags, which were identified as a total of 551 operational taxonomic units (OTUs) in all samples (Fig. 5a). This sequencing depth closely reflects the total microbial species richness. Chicks with SEBS supplementation represented 432 OTUs, the most abundant figure (Fig. 5b). All five groups are represented by 234 OTUs, contributing 42,47% of the total proportion (Fig. 5c). Bacterial compositon in pulum show a few differences with SEBS and BS supplementation (R = 0.2274). Similarities of the weighted UniFrac-based principal coordinate analysis (PCoA) indicated the mainly factors dominated 67.68% variations (Fig. 6b), which influenced the composition of mcirobiota. Results of bacterial community structure indicate that the numbers of three specific phyla of bacteria, namely *Bacteroidetes*, *Actinobacteria*, and *Epsilonbacteraeota*, significantly increased with *B. subtilis* and SEBS supplementation compared with controls, with *Actinobacteria* higher than IS and flavomycin groups (Figure S1, S2). Regarding the genus, the bacterial diversity of all supplementary groups was more abundant than controls (Figure S3, Fig. 6a). Six genera represent 87.28% of the total proportion, *Candidatus arthromitus*, *Romboutsia*, *Escherichia-Shigella*, *Enterococcus*, *Gallibacterium*, and *Tyzzerellawere*, with *Candidatus arthromitus* representing 35.54% in controls (Figure S3). Further, *Alistipes*, *Helicobacter*, *Ruminococcaceae*, and *Ruminococcus* genera were exhibited in supplementary groups, and *Lactobacillus* and *Bacteroides* were found in *B. subtilis* and SEBS groups. Similarities of PCoA showed that two main factors influenced the bacterial cluster at the genus level, indicating a ratio of 61.09% (Fig. 6b, R = 0.2545). In the PCoA of bacterial OTUs, the SEBS group samples clustered together more than any other group. Results from controls were most scattered. These suggest that the bacterial communities were most stable and optimal with SEBS supplementation.

SEBC increases organic selenium levels and GPX

The Se levels in the plasma and breast meat were measured, with the results shown in Figure S4. The results indicate that the IS group displays significantly more Se in the plasma and breast meat than the control and BS supplementation groups (*P* < 0.01). Chickens in the SEBS group exhibited the highest Se levels in both tissues (*P* < 0.01). Types of GPX, cytoplasmic (GPX1), plasma (GPX2), and gastrointestinal

(GPX4), observed in chicks were primarily antioxidative factors, containing selenium as a co-factor. The activities of GPX1, GPX2, and GPX3 were measured using ELISA assays. IS and SEBS improved the activities of GPX1, GPX2, and GPX3 compared with those without Se supplementation.

SEBS improves immunity and metabolism

The relationship between the microbiota of ileal mucous membranes and chicken body function was manifested through KEGG pathway classification and one-way ANOVA analysis. Results (Fig. 7a and 7b) indicate that more microbiota were found to promote the genetic expression of amino acids, carbohydrates, co-enzymes, lipid transport and metabolism ($P < 0.01$), energy production and conversion ($P < 0.01$), signal transduction mechanisms, and defense mechanisms ($P < 0.05$). Meanwhile, primary infectious diseases caused by pathogenic bacteria was analyzed (Fig. 7c), which showed that all four supplements strengthened defenses against bacterial invasion of chicken epithelial cells, compared to controls ($P < 0.01$). With *B. subtilis*, SEBS, and flavomycin supplementation, body defenses regarding biofilm formation against *Vibrio cholerae* improved significantly ($P < 0.01$). Further, defense against *Salmonella* infection and Pertussis improved in two *B. subtilis* and flavomycin supplementary groups (Fig. 8). Moreover, chicks receiving SEBS exhibited enhanced defense against pathogenic *Escherichia coli* infection and Shigellosis ($P < 0.01$).

Chicken immunity was regulated by intestinal bacterial composition. To unveil the relationship, we used the Spearman's correlation analysis on species of bacteria and environmental factors, BD1 levels and anti-infection, results (Fig. 8) indicated that the abundance of species of uncultured *Candidatus arthromitus* were negatively correlated with BD1 concentration and anti infection in ileal mucous membranes ($P < 0.01$), and included *Romboutsia* regarding anti-infection analysis. However, abundant species of unclassified *Lachnospiraceae*, uncultured *Anaerosporobacter*, uncultured *Ruminococcaceae_UCG-014*, uncultured *Peptococcus*, *Lactobacillus salivarius*, and unclassified *Butyricicoccus* were positively correlated with two environmental factors ($P < 0.01$). The diversity of species in all groups is shown in Figure S5 and text 1. Species of unclassified *Lachnospiraceae*, uncultured *Anaerosporobacter*, *Ruminococcaceae_UCG-014*, *Peptococcus*, *Lactobacillus salivarius*, and unclassified *Butyricicoccus* were all increased in SEBS-supplemented chicks (Fig. S4). *Lachnospiraceaer*, *Ruminococcaceae_UCG-014*, *Peptococcus*, *Lactobacillus salivarius*, and *Butyricicoccus* aid in digestion and nutrient absorption. Specifically, species of *Lactobacillus salivarius*, *Butyricicoccus*, and *Anaerosporobacter* are associated with immunity and BD1 concentration in ileal mucous membranes.

Improvement of intestinal microbiota and levels of BD1

BD1 of the innate immune system have been found in chicken intestine. BD1 was formed and secreted by small intestinal crypt cells (Fig. 9a), the protein of BD1 was transported from the intestinal crypt to villus and released from villous brush border into lumen indicated by immunohistochemical assays. A greater concentration of BD1 was secreted from the crypt of ileal mucous membranes of chicks with dietary Se, *B. subtilis*, SEBS, and flavomycin supplementation ($P < 0.01$, Fig. 9b). Chicks supplemented with IS exhibited improved secretion of BD1 ($P < 0.01$), with significant differences observed in ileum levels

compared with controls ($P < 0.01$). The levels of BD1 with *B. subtilis*, SEBS, and flavomycin were significantly higher than that of the control, while BD1 levels were highest with SEBS inclusion ($P < 0.01$, Fig. 9c).

Potential signaling pathway of SEBC

To explore the potential signaling pathway of BD1 expression regulated by SEBS, mouse primary intestinal crypt cells were cultured. The duration of proliferation of primary crypt cells reached 80% cell fusion was 48 h (Fig. 10a, 10b). Crypt cells treated with *B. subtilis*, Se-BS, and SEBS showed improved expression of BD1 than those of control and IS cells (Na_2SeO_3) (Fig. 10c, $P < 0.01$). *B. subtilis* exhibited the most robust effect on BD1 expression and several cytokines, with or without an antagonistic role. With the action of Se, expression of all measured cytokines and pro-inflammatory factors, IL-1β and TNF-α, reduced significantly compared to *B. subtilis* use alone. SEBS played a weaker role in activating the signals of IκB, IL-1β, and TNF-α than Se-BS and *B. subtilis*.

Crypt cells treated with agonists TLR2 (Pam3), TLR4 (LPS E. coli O55:B5), and TLR6 (FSL-1) for 3 h previously indicated diverse impacts on cytokines and BD1 expression. Pam3 enhanced the moderator effect of TLR2, improved the expression of BD1 compared to other agonists (Fig. S6). The expression of MyD88, IRAK, TRAF6, IκB, BD1, IL-1β, and TNF-α during Pam3 exposure appeared more enhanced than without agonist supplementation ($P < 0.01$). While the agonists LPS and TLR6 did not exert significant effects compared to that of Pam3 (Fig. S6). When crypt cells pre-treated with anti-TLR2 protein for 3 h, the expression of BD1, IL-1β, and TNF-α declined in the action of *B. subtilis*, Se-BS, and SEBS very significantly ($P < 0.01$) (Fig. 11). The expression of MyD88, IRAK, TRAF6, IκB was decreased significantly ($P < 0.05$). The treatment of Na_2SeO_3 was not influenced ($P > 0.05$).

The mouse crypt cell results indicate that the potential signaling pathway of *B. subtilis* and SEBS may originate from the recognition of TLR2 and presentation to MyD88, stimulating and provoking downstream signals of IRAK, TRAF6, IκB, IL-1β, and TNF-α. Experiments conducted in mouse crypt cells indicate that the recognized receptor was TLR2, and the signaling pathway is the classic TLR2-MyD88-NF-kB pathway.

The signaling molecules in the chick ileum were further inspected using qRT-PCR. The mRNA expression of cytokines *BD1, TLR2, IL-1β, TNF-α, IL-6, IFN-γ*, and *NF-kB1* were monitored (Fig. S7), with increased expression of all cytokines observed in in SEBS, BS, and flavomycin groups, compared to controls ($P < 0.01$). In the IS-supplemented group, the expression of BD1 and IFN-γ were significantly improved compared with control groups ($P < 0.01$). The expression of cytokines IL-1β, TNF-α, IL-6, and IFN-γ in the *B. subtilis* group was higher than those observed in the SEBS group ($P < 0.01$). Cytokines IL-1β, TNF-α, IL-6, and IFN-γ were also pro-inflammatory factors, which easily induce inflammation. With the action of Se, the expression of three pro-inflammatory factors was significantly reduced.

Discussion

In order to explore the combined effect of Se and *B. subtilis*, we first cultured the SEBS, then analyzed its morphological and biochemical characteristics. These characteristics did not exhibit any differences compared to *B. subtilis* after being bio-transformed with inorganic Se. Selenomethionine was proved as the primary ionic form of selenium in bacteria after fermentation [31]. The ionic form of Se in the supernatant and precipitate of fermented SEBS medium constituted nano-selenium in red particles [32]. Hence, the composition of Se in the supernatant and precipitate of fermented SEBS medium was mainly as selenomethionine and nano-selenium in red particles, which confers a pale pink color to the medium. The valences of Se changed from 4 + into 2- and 0. Then, Chinese Huainan Partridge chickens were supplemented with SECB, to unveil the effect on intestinal innate immune expression of BD1 and its potential mechanism.

Chicks exhibited higher final body weights in the chicken study with *B. subtilis* and SEBS supplementation. The promoting effect on growth was also shown in the final body weight of the *B. subtilis*, SEBS, and flavomycin groups. This result was conformed with previous study [33, 34]. Both Se and *B. subtilis* modulate the growth performance of chickens [35, 36]. However, we did not observe any significant effects of IS supplementation. In our study, we supplemented basal feedstuff with a dose of 0.5 μg/g Se in an inorganic form, which had no positive effects on Chinese Huainan Partridge chickens; this is in accordance with our previous studies [2, 3, 37].

Exploring the colonization of bacteria *in vivo* must be more eloquent than in cells *in vitro. B. subtilis* fed to chicks can colonize in the ileal mucous membranes, the bacterial number was ascertained using FISH and qRT-PCR assays. The bacteria used nutrients in the intestine, ingested by the chick, for propagation, while conferring health benefits to the chick indicating a reciprocal relationship [38, 39]. With bacterial growth, metabolites of *B. subtilis* include antimicrobial substances, digestive enzymes, such as protease, lipase, and amylase, which play important roles in maintaining health and breaking down feedstuff for nutrient absorption [40]. Chickens receiving SEBS exhibited a higher final body weight and greater feed utilization efficiency than control chickens, compared with the group receiving *B. subtilis*, suggesting that this treatment was more efficient in regulating growth for the biological roles of Se than *B. subtilis* alone. SEBS combined the merits of Se and *B. subtilis* to improve growth performance of chicks.

One benefit of *B. subtilis* is represented by improving the development of intestinal stem cells, such as promoting the development of intestinal stem cells, increasing the villous height of the small intestine, and decreasing crypt depth [33, 41]. Accompanied with the colonization of *B. subtilis*, immunity was also improved through such reciprocal pathways [39]. The results of immunohistochemical assays showed that BD1 is secreted in the small intestinal crypt and stimulated with *B. subtilis* and SEBS colonization, which improved innate immunity to defend against infection by endogenous pathogenic or conditioned pathogenic bacteria [6, 15]. The colonization of *B. subtilis* in the ileal mucous membrane enriched bacterial diversity, which improved the phylum and genus of bacterial composition. Genera of *lactobacillus*, *Peptococcus*, *Butyricicoccus*, and *Ruminococcaceae_UCG-014* serve probiotic functions for the body, and the proportion of these bacteria increased in chicks receiving *B. subtilis* and SEBS supplementation [42–44]. Meanwhile, the ration of conditioned pathogens or pathogens, such as

Escherichia-Shigella, *Vibrio cholerae*, *Salmonella*, and *Pertussis bacilli*, significantly declined. Improved immunity can be indirectly attributed to these results. Abundant species of unclassified *Lachnospiraceae*, uncultured *Anaerosporobacter*, uncultured *Ruminococcaceae_UCG-014*, uncultured *Peptococcus*, *Lactobacillus salivarius*, and unclassified *Butyricicoccus* can be detected in *B. subtilis* and SEBS groups. The species of *Lachnospiraceaer*, *Ruminococcaceae_UCG-014*, *Peptococcus*, *Lactobacillus salivarius*, *Butyricicoccus*, and *Anaerosporobacter* improved overall health [45–48]. KEGG Ortholog (KO) functional profiles of microbial communities indicated that metabolism and immunity were improved by these species of bacteria.

Body immunity was improved by optimized intestinal microbiota. BD1 as an important component of innate immune, to determine the mechanism of BD1 expression regulated by SEBS is urgent. We first explored the potential signaling pathway of *B. subtilis* and SEBS on mouse ileal crypt cells, then chicken crypt cells were employed. The innate immune system initiates a response to microorganisms via pattern recognition receptors, which have been extensively studied to explain the regulatory effects of immunobiotic bacteria in both immune and intestinal epithelial cells [49]. TLRs play a critical role in the recognition of pathogens by the innate immune system [50]. Individual TLRs recognize distinct components of microorganisms. The TLRs primarily responsible for recognition of gram-positive bacteria are TLR 2, 4, and 6 [13]. Results of mouse ileal crypt cells treated with agonists Pam3, LPS, and FSL-1 showed varying influences on target signal molecular expression. No differences were observed regarding the function of agonists LPS and FSL-1, compared with non-supplementation. However, with the action of Pam3, the classic TLR2 signaling pathway was stimulated under the influence of *B. subtilis* and SEBS, which indicates that *B. subtilis* was recognized by TLR2, as opposed to TLR4 and 6. In further, the mouse crypt cells pretreated with anti-TLR2 protein, the down-stream signaling pathway was inhibited. These results suggested that the TLR2 was the recognized receptor of *B. subtilis*. TLR2 is an important PRR that plays an essential role in immune regulation by probiotics. It has a broad recognition profile that includes products from gram-positive bacteria, including lipoteichoic acid, peptidoglycan, lipoproteins [50, 51]. *B. subtilis* and SEBS as gram-positive bacteria adhered to ileal mucous membrane as an integrated whole, which were recognized by TLR2 and presented into downstream. The signal was presented downstream to MyD88, IRAK, TRAF6, IκB, BD1, IL-1β, TNF-α, and IL-6 [14, 52], which resulted in nuclear localization and stimulated nuclear factor kappa B1-induced expression of BD1 protein. The TLRs-NF-kB1 pathway represents the classic signaling pathway in cells, which was studied and discovered in molecular biology research [52–54]. Our results proved that the same TLR2-MyD88-NF-kB1 pathway recognized SEBS to evoke BD1 expression. In addition, whether TLR2 exerts its actions by forming heterodimers with other TLRs namely TLR1 or TLR6 [55, 56] and cooperating with TLR2 coreceptors remains to be investigated.

B. subtilis and SEBS inoculated in mouse crypt cells stimulated cellular immune inflammation, leading to increased expression of pro-inflammatory factors, such as IL-1β, TNF-α, and IL-6. Supplementary dose of 0.125 μg/mL Se in culture medium could downregulate the inflammation caused by *B. subtilis* infection [57]. The same results could be found in chicken ileum, with decreased expression of IL-1β, TNF-α, IL-6, and IFN-γ. While BD1 levels in vivo were higher in SEBS than that of *B. subtilis*, which was attributed to

selenium functionality. In mouse crypt cells, the combined use of Na_2SeO_3 and *B. subtilis* could reduce inflammation, this reduction was lower than that of SECB, which suggested that the benefits were magnified with combined use of Se bio-conversion by *B. subtilis* as SECB.

The supplementation of Se also enhanced the bacterial diversity of the ileum. SEBS, due to the effects of *B. subtilis* and Se, exerted a more robust effect. Previous studies have reported that Se supplementation can increase Se tissue content, although the results varied [58]. In our study, the Se contents in the plasma and liver increased significantly in the IS and SEBS groups, which indicated that the dietary supplement containing Se exerted a significant influence on the Se level; this is in accordance with previous reports [37, 57]. The effect of SEBS was greater than that of IS in this experiment, suggesting that Se availability was greater with SEBS supplementation. Meanwhile, the activities of cytoplasmic, plasma, and gastrointestinal GPX in chicks were enhanced with Se supplementation, which is helpful to overcome the stress caused by cold temperatures and other stressors [28]. Se supplementation enriched the bacterial diversity compared to controls, which enhanced nutrient metabolism and immunity, as indicated by results of KEGG function classification. Further, the expression of cytokines in mouse and chicken intestinal cells indicated that TNF-α, IFN-γ and BD1 expression increased. Selenium improved the body immunity and alleviated the inflammatory response meanwhile [59]. Both the qPCR results of mouse and chicken crypt cells suggested that the pro-inflammatory factors IL-1β, TNF-α, IL-6, and IFN-γ declined in combined use of *B. subtilis* and Se than single use of *B. subtilis*. And the inhibition of TLR2 led to decreased expression of alleviated roles. All of these advised that Se was partly through recognition of TLRs and presentation to the signaling pathway TLR2-NF-kB1 to affect the expression of cytokines as well as seleno-protein [22, 60, 61]. Se absorbed and deposited in organism as compound substances such as seleno-protein alleviate the bodily inflammatory response through TLRs recognized may be influenced by the recognition of pro-inflammatory substances combined such as lipopolysaccharide or pathogen by certain TLRs. Ionic Se was transformed into organic Se and nano Se when culture with *B. subtilis*. Se in body of *B. subtilis* as SECB mainly as seleno-protein bounded with peptidoglycan, spore was recognized by TLR2 of intestinal crypt cells and activate the immune response.

Conclusion

In this study, we cultured selenium enriched *B. subtilis* (SEBS). Thereafter, SEBS was added to the diet of chicks to determine its effect on growth and immunity. A representative graphical model is shown in Fig. 1. Our study first reported the colonization of probiotic bacteria *B. subtilis* in the bodily intestine using FISH and qRT-PCR. Thereafter, we observed that the composition of intestinal microbiota and immunity were improved under the interplay of colonization. BD1 as an important innate immune component, the potential signaling pathway of SEBS was proposed to be TLR2-MyD88NF-kB1. Se binding to the body of *B. subtilis* can reduce the inflammatory response of intestinal crypt cells and promote the immunity and anti oxidation. Combined use of Se and *B. subtilis* as SEBS induced further improvements compared to those observed when administered alone. Our research provided a new avenue in use of probiotics and essential micro-elements.

Declarations

Ethics approval and consent to participate

The experimental protocols in this study including animal husbandry and slaughter were approved by the Institution of Animal Science and Welfare of Anhui Province (no. IASWAP2017110649).

Consent for publication

Not applicable

Availability of data and materials

The data supporting the conclusions of this article are included within the article.

Competing interests

All of authors declare no conflicts of interest.

Funding

This investigation was supported by the National Natural Science Foundation of China (31772811, and 31602123), the fund of the Key National Research and Development Program project of China (2016YFD0500703), the fund of scientific and technological innovation team of Anhui Academy of Agricultural Sciences (No. 2020YL036), Anhui poultry industry technology system project (No. AHCYTX-6) and Anhui Academy of Agricultural Sciences Key Laboratory Project (No.2020YL031).

Authors' contributions

HK conceived the idea of the study. YJ carried out animal experiment, data analysis, and drafted the

manuscript. ZM and WJ did the cell culture, YP and LZ analyzed the qRT-PCR of cells. ZK, WD and WY took part in samples collection. WZ, WC and HK revised the manuscript.

Acknowledgements

We would like to thank Editage (www.editage.cn) for English language editing.

References

1. Hill C, Guarner F, Reid G, Gibson GR, Merenstein DJ, Pot B, Morelli L, Canani RB, Flint HJ, Salminen S, Calder PC, Sanders ME. Expert consensus document. The International Scientific Association for Probiotics and Prebiotics consensus statement on the scope and appropriate use of the term probiotic. Nat Rev Gastroenterol Hepatol. 2014;11(8):506–14.

2. Yang JJ, Qian K, Wu D, Zhang W, Wu YJ, Xu YY. Effects of different proportions of two *Bacillus* strains on the growth performance, small intestinal morphology, caecal microbiota and plasma biochemical profile of Chinese Huainan Partridge Shank chickens. J Integr Agr. 2017;16(6):1383–92.
3. Yang J, Zhang M, Zhou Y. Effects of selenium-enriched *Bacillus* sp. compounds on growth performance, antioxidant status, and lipid parameters breast meat quality of Chinese Huainan partridge chicks in winter cold stress. Lipids Health Dis. 2019;18(1):63.
4. Lynn DJ, Higgs R, Gaines S, Tierney J, James T, Lloyd AT, Fares MA, Mulcahy G, O'Farrelly C. Bioinformatic discovery and initial characterisation of nine novel antimicrobial peptide genes in the chicken. Immunogenetics. 2004;56(3):170–7.
5. van Dijk A, Veldhuizen EJ, Kalkhove SI, Tjeerdsma-van Bokhoven JL, Romijn RA, Haagsman HP. The beta-defensin gallinacin-6 is expressed in the chicken digestive tract and has antimicrobial activity against food-borne pathogens. Antimicrob Agents Chemother. 2007;51(3):912–22.
6. Bar-Shira E, Friedman A. Development and adaptations of innate immunity in the gastrointestinal tract of the newly hatched chick. Dev Comp Immunol. 2006;30(10):930–41.
7. Cadwell K, Niranji SS, Armstrong VL, Mowbray CA, Bailey R, Watson KA, Hall J. AvBD1 nucleotide polymorphisms, peptide antimicrobial activities and microbial colonisation of the broiler chicken gut. BMC Genom. 2017;18(1):637.
8. Singh PK, Jia HP, Wiles K, Hesselberth J, Liu L, Conway BA, Greenberg EP, Valore EV, Welsh MJ, Ganz T, Tack BF, McCray PB Jr. Production of beta-defensins by human airway epithelia. Proc Natl Acad Sci USA. 1998;95(25):14961–6.
9. Taggart CC, Greene CM, Smith SG, Levine RL, McCray PB Jr, O'Neill, McElvaney S. NG. Inactivation of human beta-defensins 2 and 3 by elastolytic cathepsins. J Immunol. 2003;171(2):931–7.
10. Ryan LK, Wu J, Schwartz K, Yim S, Diamond G. β-Defensins coordinate in vivo to inhibit bacterial infections of the trachea. Vaccines (Basel). 2018;6(3). pii: E57.
11. Tomalka J, Azodi E, Narra HP, Patel K, O'Neill S, Cardwell C, Hall BA, Wilson JM, Hise AG. β-Defensin 1 plays a role in acute mucosal defense against Candida albicans. J Immunol. 2015;194(4):1788–95.
12. Harwig SS, Swiderek KM, Kokryakov VN, Tan L, Lee TD, Panyutich EA, Aleshina GM, Shamova OV, Lehrer RI. Gallinacins: cysteine-rich antimicrobial peptides of chicken leukocytes. FEBS Lett. 1994;342(3):281–5.
13. Akira S, Hemmi H. Recognition of pathogen-associated molecular patterns by TLR family. Immunol Lett. 2003;85(2):85–95.
14. Awane M, Andres PG, Li DJ, Reinecker HC. NF-kappa B-inducing kinase is a common mediator of IL-17-, TNF-alpha-, and IL-1 beta-induced chemokine promoter activation in intestinal epithelial cells. J Immunol. 1999;162(9):5337–44.
15. Hancock RE, Diamond G. The role of cationic antimicrobial peptides in innate host defences. Trends Microbiol. 2000;8(9):402–10.
16. Scott MG, Hancock RE. Cationic antimicrobial peptides and their multifunctional role in the immune system. Crit Rev Immunol. 2000;20(5):407–31.

17. Harvey SA, Romanowski EG, Yates KA, Gordon YJ. Adenovirus-directed ocular innate immunity: the role of conjunctival defensin-like chemokines (IP-10, I-TAC) and phagocytic human defensin-alpha. Invest Ophthalmol Vis Sci. 2005;46(10):3657–65.
18. Nicholson WL. Roles of *Bacillus* endospores in the environment. Cell Mol Life Sci. 2002;59:410–6.
19. Liotta D, Monahan R III. Selenium in organic synthesis. Science. 1986;231(4736):356–61.
20. Brown KM, Arthur JR. Selenium, selenoproteins and human health: a review. Public Health Nutr. 2001;4(2B):593–9.
21. Gan F, Hu Z, Huang Y, Xue H, Huang D, Qian G, Hu J, Chen X, Wang T, Huang K. Overexpression of pig selenoprotein S blocks OTA-induced promotion of PCV2 replication by inhibiting oxidative stress and p38 phosphorylation in PK15 cells. Oncotarget. 2016;7(15):20469–85.
22. Hao S, Hu J, Song S, Huang D, Xu H, Qian G, Gan F, Huang K. Selenium alleviates aflatoxin Bâ-induced immune toxicity through improving glutathione peroxidase 1 and selenoprotein S Expression in primary porcine splenocytes. J Agric Food Chem. 2016;64(6):1385–93.
23. El-Boshy ME, Risha EF, Abdelhamid FM, Mubarak MS, Hadda TB. Protective effects of selenium against cadmium induced hematological disturbances, immunosuppressive, oxidative stress and hepatorenal damage in rats. J Trace Elem Med Biol. 2015;29:104–10.
24. Yi J, Cheng J. Effects of water chemistry and surface contact on the toxicity of silver nanoparticles to *Bacillus subtilis*. Ecotoxicology. 2017;26(5):639–47.
25. National Research Council. Nutrient requirements of poultry. 11th rev. ed. National Academy Press, Washington DC, USA, 2012.
26. Blanco G, Díaz de Tuesta JA. Culture- and molecular-based detection of swine-adapted *Salmonella* shed by avian scavengers. Sci Total Environ. 2018;634:1513–8.
27. Mountzouris KC, Tsitrsikos P, Palamidi I, Arvaniti A, Mohnl M, Schatzmayr G, Fegeros K. Effects of probiotic inclusion levels in broiler nutrition on growth performance, nutrient digestibility, plasma immunoglobulins, and cecal microflora composition. Poult Sci. 2010;89(1):58–67.
28. Brown KM. Pickard K, Nicol F, Beckett GJ, Duthie GG, Arthur JR. Effects of organic and inorganic selenium supplementation on selenoenzyme activity in blood lymphocytes, granulocytes, platelets and erythrocytes. Clin Sci (Lond). 2000;98(5):593–9.
29. Pistón M, Silva J, Pérez-Zambra R, Dol I, Knochen M. Automated method for the determination of total arsenic and selenium in natural and drinking water by HG-AAS. Environ Geochem Health. 2012;34(2):273–8.
30. Battin C, Hennig A, Mayrhofer P, Kunert R, Zlabinger GJ, Steinberger P, Paster W. A human monocytic NF-κB fluorescent reporter cell line for detection of microbial contaminants in biological samples. PLoS One. 2017;12(5):e0178220.
31. Gao J, Huang K, Qin S. Determination of selenomethionine in selenium-enriched yeast by gas chromatography-mass spectrometry. Se Pu. 2006;24(3):235–8.

32. Wang Y, Shu X, Zhou Q, Fan T, Wang T, Chen X, Li M, Ma Y, Ni J, Hou J, Zhao W, Li R, Huang S, Wu L. Selenite reduction and the biogenesis of selenium nanoparticles by *alcaligenes faecalis* Se03 Isolated from the Gut of Monochamus alternatus (Coleoptera: Cerambycidae). Int J Mol Sci. 2020;21(4):E1294.
33. Park JH, Kim IH. The effects of the supplementation of *Bacillus subtilis* RX7 and B2A strains on the performance, blood profiles, intestinal Salmonella concentration, noxious gas emission, organ weight and breast meat quality of broiler challenged with Salmonella typhimurium. J Anim Physiol Anim Nutr (Berl). 2015;99(2):326–34.
34. Bai K, Huang Q, Zhang J, He J, Zhang L, Wang T. Supplemental effects of probiotic *Bacillus subtilis* fmbJ on growth performance, antioxidant capacity, and meat quality of broiler chickens. Poult Sci. 2017;96(1):74–82.
35. Yang J, Xu Y, Qian K, Zhang W, Wu D, Wang C. Effects of chromium enriched *Bacillus subtilis* KT260179 supplementation on growth performance, caecal microbiology, tissue selenium level, insulin receptor expression and plasma biochemical profile of mice under heat stress. Br J Nutr. 2016;15:774–81.
36. Han XJ, Qin P, Li WX, Ma QG, Ji C, Zhang JY, Zhao LH. Effect of sodium selenite and selenium yeast on performance, egg quality, antioxidant capacity, and selenium deposition of laying hens. Poult Sci. 2017;96:3973–80.
37. Yang JJ, Huang KH, Qin SY, Wu XS, Zhao ZP, Chen F. Antibacterial action of selenium-enriched probiotics against pathogenic Escherichia coli. Dig Dis Sci. 2009;54:246–54.
38. Yang J, Qian K, Wang C, Wu Y. Roles of Probiotic lactobacilli inclusion in helping piglets establish healthy intestinal inter-environment for pathogen defense. Probiotics Antimicrob Proteins. 2018;10(2):243–50.
39. Maynard CL, Elson CO, Hatton RD, Weaver CT. Reciprocal interactions of the intestinal microbiota and immune system. Nature. 2012;489(7415):231–41.
40. Ohno A, Ano T, Shoda M, Effect of temperature on production of lipopeptide antibiotics, iturin A and surfactin by a dual producer, *Bacillus subtilis* RB14, in solid-state fermentation. Journal of Fermentation and Bioengineering. 1995;80:517–519.
41. Biton M, Haber AL, Rogel N, Burgin G, Beyaz S, Schnell A, Ashenberg O, Su CW, Smillie C, Shekhar K, Chen Z, Wu C, Ordovas-Montanes J, Alvarez D, Herbst RH, Zhang M, Tirosh I, Dionne D, Nguyen LT, Xifaras ME, Shalek AK, von Andrian UH, Graham DB, Rozenblatt-Rosen O, Shi HN, Kuchroo V, Yilmaz OH, Regev A, Xavier RJ. T helper cell cytokines modulate intestinal stem cell renewal and differentiation. Cell. 2018;175(5):1307–20.
42. Pan F, Zhang L, Li M, Hu Y, Zeng B, Yuan H, Zhao L, Zhang C. Predominant gut *Lactobacillus murinus* strain mediates anti-inflammaging effects in calorie-restricted mice. Microbiome. 2018;6(1):54.
43. Eeckhaut V, Machiels K, Perrier C, Romero C, Maes S, Flahou B, Steppe M, Haesebrouck F, Sas B, Ducatelle R, Vermeire S, Van Immerseel F. *Butyricicoccus pullicaecorum* in inflammatory bowel disease. Gut. 2013;62(12):1745–52.

44. Zhang C, Zhang M, Pang X, Zhao Y, Wang L, Zhao L. Structural resilience of the gut microbiota in adult mice under high-fat dietary perturbations. ISME J. 2012;6(10):1848–57.
45. Zeng H, Larson KJ, Cheng WH, Bukowski MR, Safratowich BD, Liu Z, Hakkak R. Advanced liver steatosis accompanies an increase in hepatic inflammation, colonic, secondary bile acids and *Lactobacillaceae/ Lachnospiraceae* bacteria in C57BL/6 mice fed a high-fat diet. J Nutr Biochem. 2020;78:108336.
46. Hu L, Jin L, Xia D, Zhang Q, Ma L, Zheng H, Xu T, Chang S, Li X, Xun Z, Xu Y, Zhang C, Chen F, Wang S. Nitrate ameliorates dextran sodium sulfate-induced colitis by regulating the homeostasis of the intestinal microbiota. Free Radic Biol Med. 2019;S0891-5849(19)31288-2.
47. Shrestha N, Sleep SL, Cuffe JSM, Holland OJ, McAinch AJ, Dekker Nitert M, Hryciw DH. Pregnancy and diet-related changes in the maternal gut microbiota following exposure to an elevated linoleic acid diet. Am J Physiol Endocrinol Metab. 2020;318(2):E276–85.
48. Zhu W, Gregory JC, Org E, Buffa JA, Gupta N, Wang Z, Li L, Fu X, Wu Y, Mehrabian M, Sartor RB, McIntyre TM, Silverstein RL, Tang WHW, DiDonato JA, Brown JM, Lusis AJ, Hazen SL. Gut microbial metabolite TMAO enhances platelet hyperreactivity and thrombosis risk. Cell. 2016;165(1):111–24.
49. Kanmani P, Albarracin L, Kobayashi H, Iida H, Komatsu R, Humayun Kober AKM, Ikeda-Ohtsubo W, Suda Y, Aso H, Makino S, Kano H, Saito T, Villena J, Kitazawa H. Exopolysaccharides from *Lactobacillus delbrueckii* OLL1073R-1 modulate innate antiviral immune response in porcine intestinal epithelial cells. Mol Immunol. 2018;93:253–65.
50. Zähringer U, Lindner B, Inamura S, Heine H, Alexander C. TLR2 - promiscuous or specific? A critical re-evaluation of a receptor expressing apparent broad specificity. Immunobiology. 2008;213:205–24.
51. Nilsen NJ, Deininger S, Nonstad U, Skjeldal F, Husebye H, Rodionov D, von Aulock S, Hartung T, Lien E, Bakke O, Espevik T. Cellular trafficking of lipoteichoic acid and Toll-like receptor 2 in relation to signaling: role of CD14 and CD36. J Leukoc Biol. 2008;84(1):280–91.
52. Mookherjee N, Brown KL, Bowdish DM, Doria S, Falsafi R, Hokamp K, Roche FM, Mu R, Doho GH, Pistolic J, Powers JP, Bryan J, Brinkman FS, Hancock RE. Modulation of the TLR-mediated inflammatory response by the endogenous human host defense peptide LL-37. J Immunol. 2006;176(4):2455–64.
53. Karin M, Lawrence T, Nizet V. Innate immunity gone awry: linking microbial infections to chronic inflammation and cancer. Cell. 2006;124(4):823–35.
54. Yarandi SS, Kulkarni S, Saha M, Sylvia KE, Sears CL, Pasricha PJ. Intestinal bacteria maintain adult enteric nervous system and nitrergic neurons via Toll-like Receptor 2-induced neurogenesis in mice. Gastroenterology. 2020;S0016-5085(20):30404–2.
55. Jin MS, Kim SE, Heo JY, Lee ME, Kim HM, Paik SG, Lee H, Lee JO. Crystal structure of the TLR1-TLR2 heterodimer induced by binding of a tri-acylated lipopeptide. Cell. 2007 Sep 21;130(6):1071-82.
56. Wang W, Deng Z, Wu H, Zhao Q, Li T, Zhu W, Wang X, Tang L, Wang C, Cui SZ, Xiao H, Chen J. A small secreted protein triggers a TLR2/4-dependent inflammatory response during invasive Candida albicans infection. Nat Commun. 2019 Mar 4;10(1):1015.

57. Wu X, Huang K, Wei C, Chen F, Pan C. Regulation of cellular glutathione peroxidase by different forms and concentrations of selenium in primary cultured bovine hepatocytes. J Nutr Biochem. 2010;21(2):153–61.
58. Prescha A, Krzysik M, Zablocka-Slowinska K, Grajeta H. Effects of exposure to dietary selenium on tissue mineral contents in rats fed diets with fiber. Biol Trace Elem Res. 2014;159:325–31.
59. Li MY, Gao CS, Du XY, Zhao L, Niu XT, Wang GQ, Zhang DM. Effect of sub-chronic exposure to selenium and astaxanthin on Channa argus: Bioaccumulation, oxidative stress and inflammatory response. Chemosphere. 2020;244:125546.
60. Chen Y, Zhao YF, Yang J, Jing HY, Liang W, Chen MY, Yang M, Wang Y, Guo MY. Selenium alleviates lipopolysaccharide-induced endometritis via regulating the recruitment of TLR4 into lipid rafts in mice. Food Funct. 2020;11(1):200–10.
61. Hou L, Zhou X, Gan F, Liu Z, Zhou Y, Qian G, Huang K. Combination of selenomethionine and N-acetylcysteine alleviates the joint toxicities of aflatoxin B1 and ochratoxin A by ERK MAPK signal pathway in porcine alveolar Macrophages. J Agric Food Chem. 2018;66(23):5913–23.

Figures

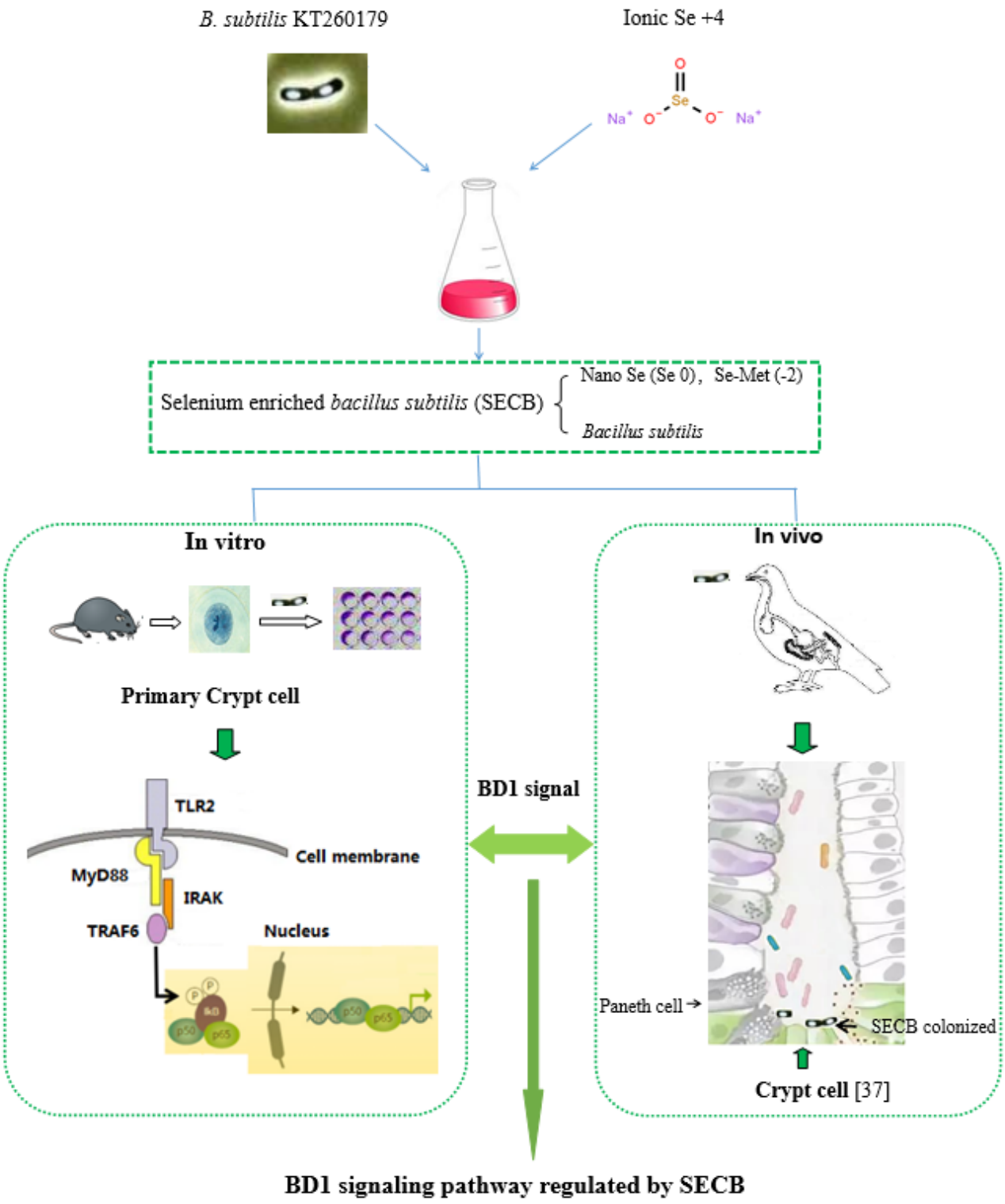

Figure 1

The graphical conclusion of the SECB on expression of BD1.

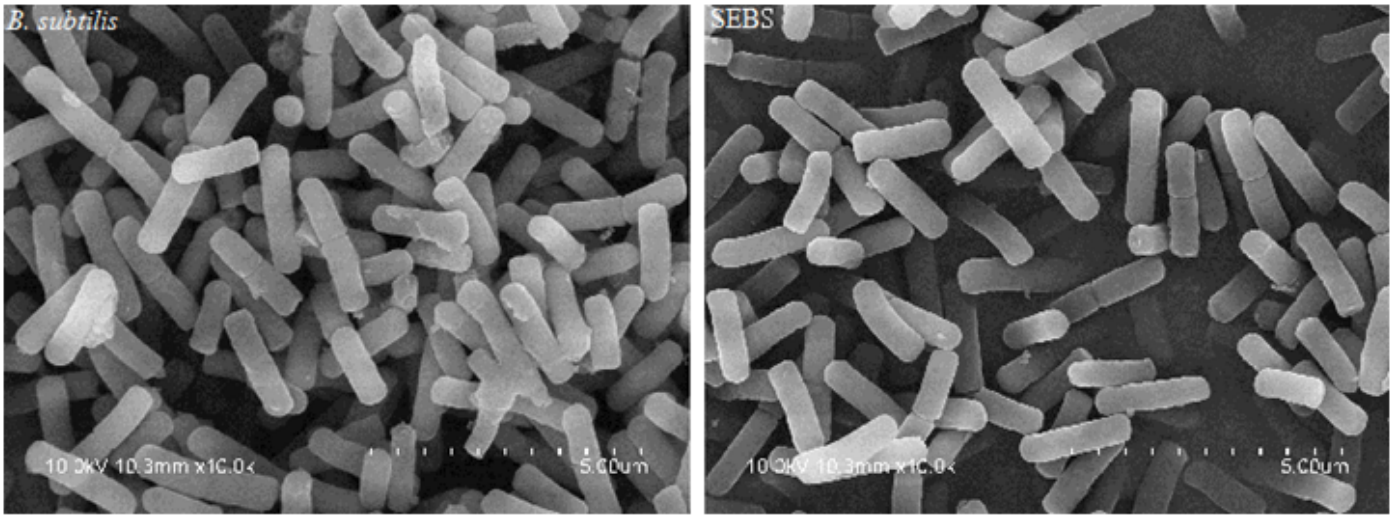

Fig. 2a The morphologic of *B. subtilis* and SEBS (×10000 magnification)

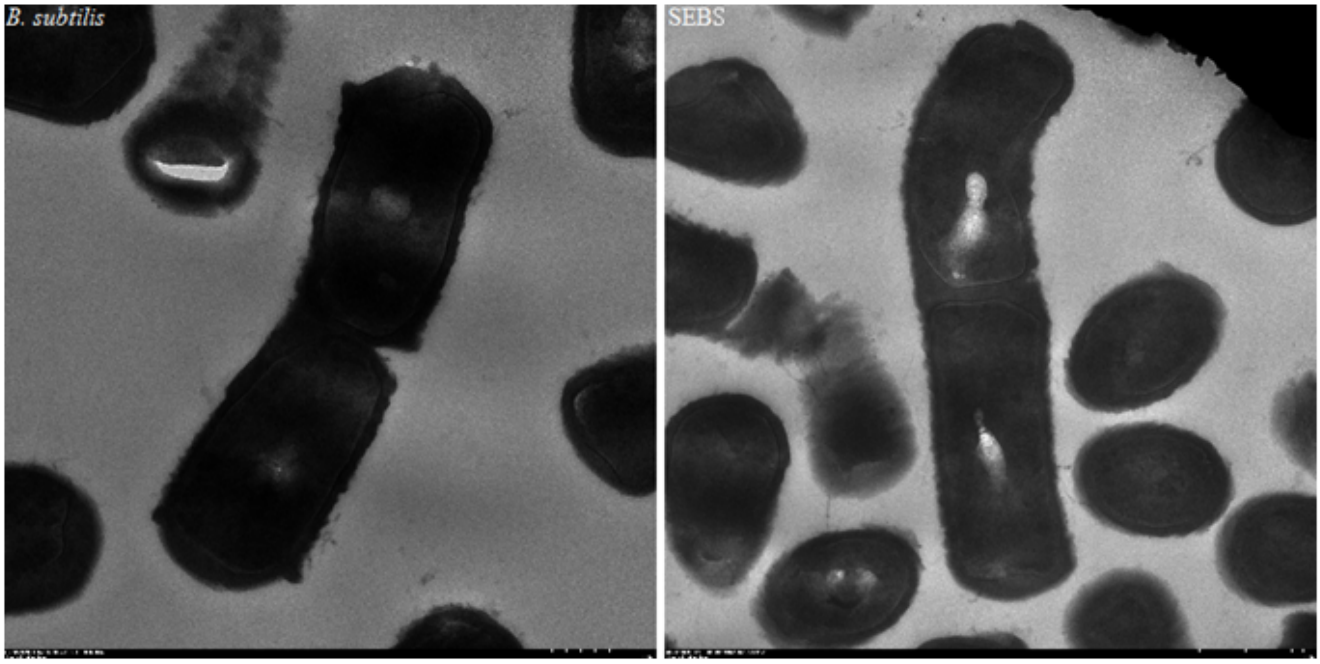

Fig. 2b The structure of *B. subtilis* and SEBS S (×10000 magnification).

Figure 2

The morphologic and structural properties of bacteria between B. subtilis and SECB. Fig. 2a The morphologic of B. subtilis and SEBS (×10000 magnification). Fig. 2b The structure of B. subtilis and SEBS (×10000 magnification).

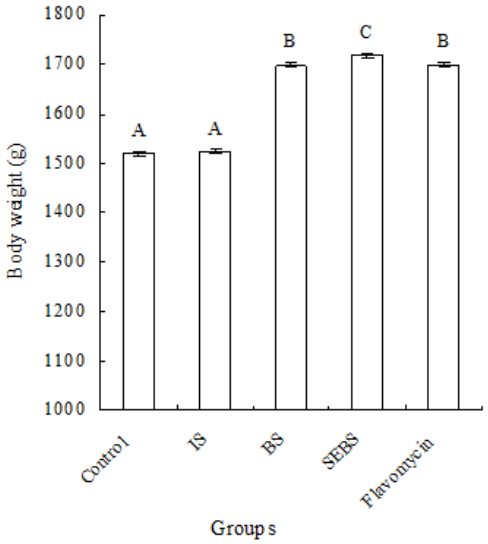

Fig. 3a Growth performance of different groups.

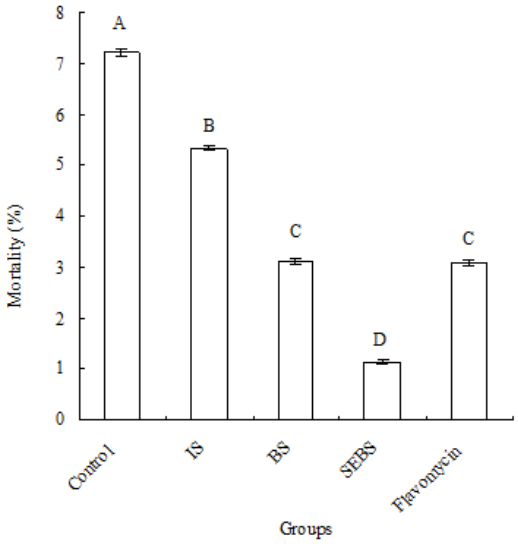

Fig. 3b Mortality of different groups.

Figure 3

Growth performance and mortality. Fig. 3a Growth performance of different groups. Fig. 3b Mortality of different groups. Data was statistically processed as repeated measurements. The different superscript capital letters in the same color of column in the same experimental duration mean significant difference at 0.01 levels ($P<0.01$).

Figure 4 Colonization of measured bacteria of different groups with FISH and qRT-PCR assay.

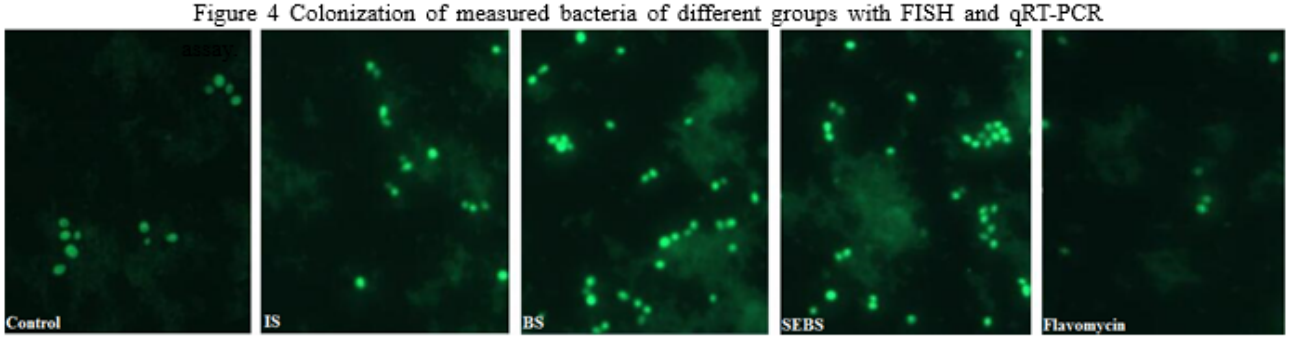

Fig. 4a Colonization of *B. subtilis* in the distal ileum measured with FISH.

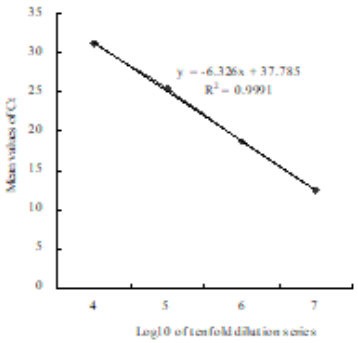

Fig. 4b The standard curve of *B. subtilis*.

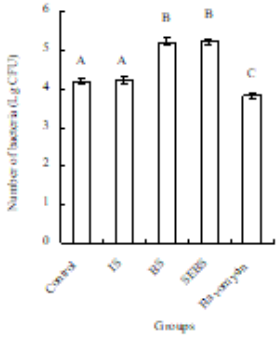

Fig. 4c Number of Colonized *B. subtilis*.

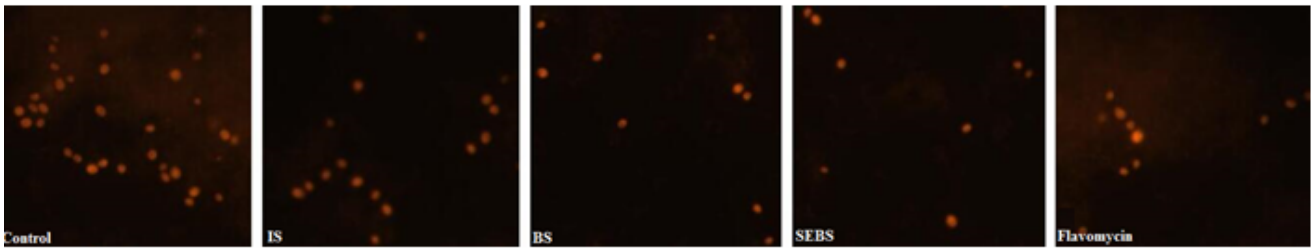

Fig. 4d Colonization of endogenous *Salmonella* in the distal ileum of different groups.

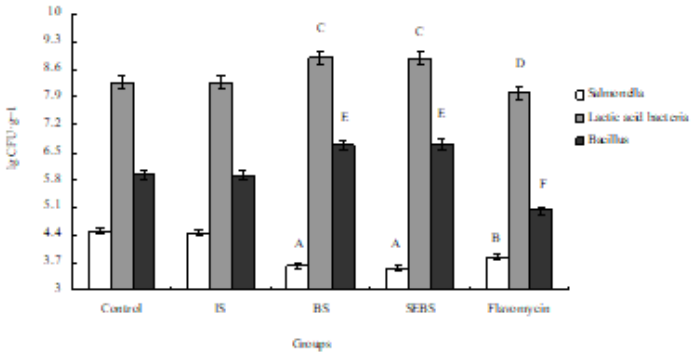

Fig. 4e Number of native bacteria in the ileal mucous membrane.

Figure 4

Colonization of measured bacteria of different groups with FISH and qRT-PCR assay. Fig. 4a Colonization of B. subtilis in the distal ileum measured with FISH. Fig. 4b The standard curve of B. subtilis. Fig. 4c Number of Colonized B. subtilis. Fig. 4d Colonization of endogenous Salmonella in the distal ileum of different groups. Fig. 4e Number of native bacteria in the ileal mucous membrane. Values are means, with standard errors are represented by vertical bars. Mean value was significantly different from that of

the control group by one-way ANOVA followed by Tukey's multiple comparison tests: the different superscript capital letters in the same color of column in the same experimental duration mean significant difference at 0.01 levels (P<0.01).

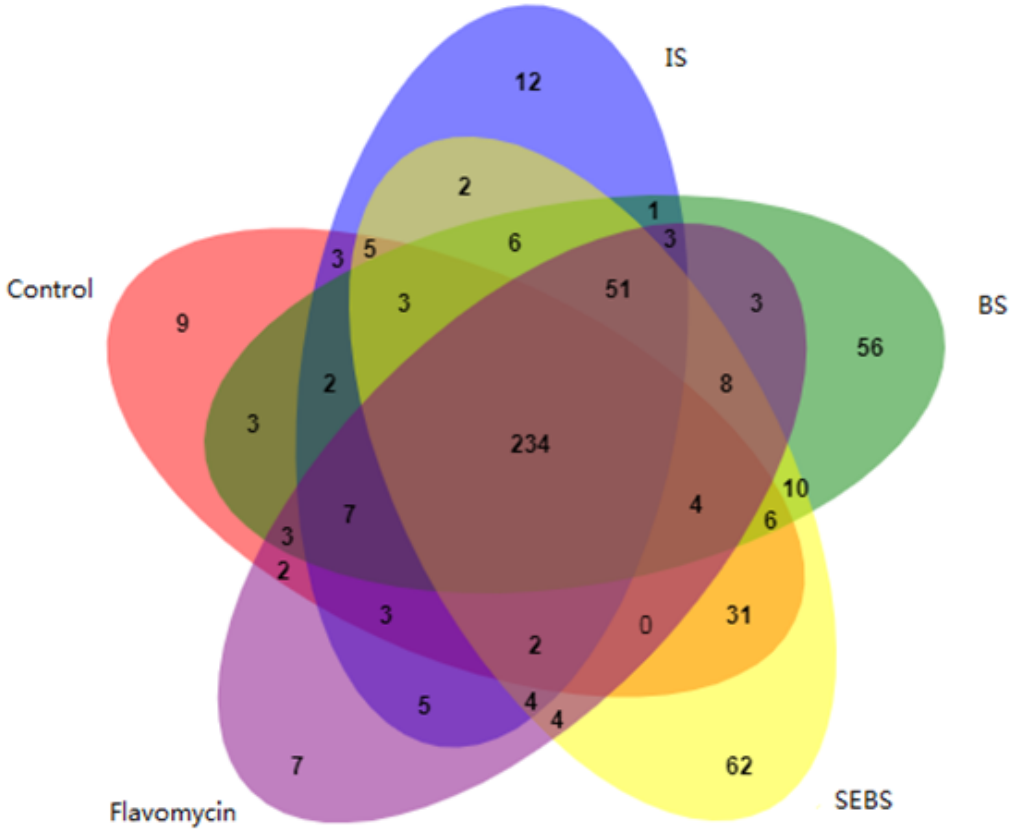

Fig. 5a The size of OTU in each groups.

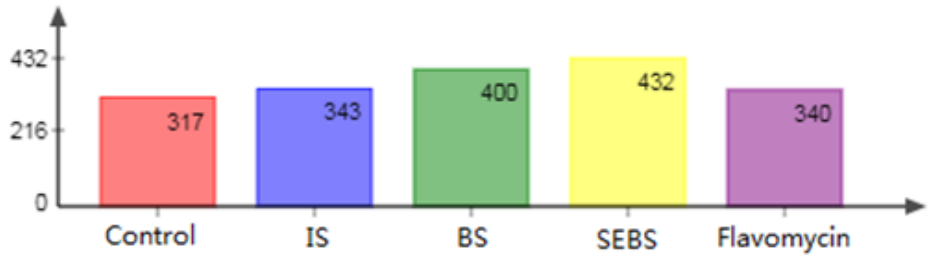

Fig. 5b The number of OTU in each groups.

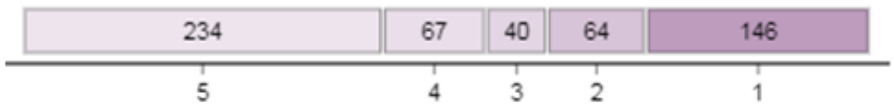

Fig. 5c Number of elements shared by 5, 4, 3, 2 or 1 groups.

Figure 5

The composition of bacterial OTU in ileal mucous membrane (Venn figures). Fig. 5a The size of OTU in each groups. Fig. 5b The number of OTU in each groups. Fig. 6c Number of elements shared by 5, 4, 3, 2

or 1 groups.

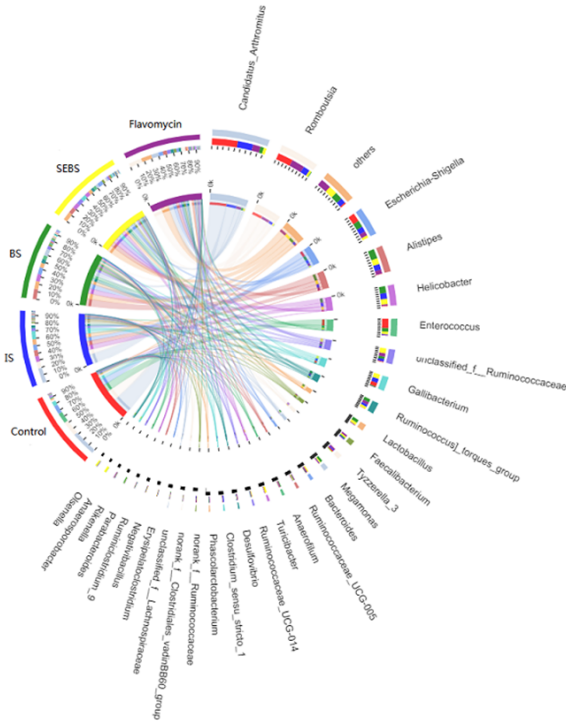

Fig 6a The Circos figure of relationship between bacterial composition (genus level).

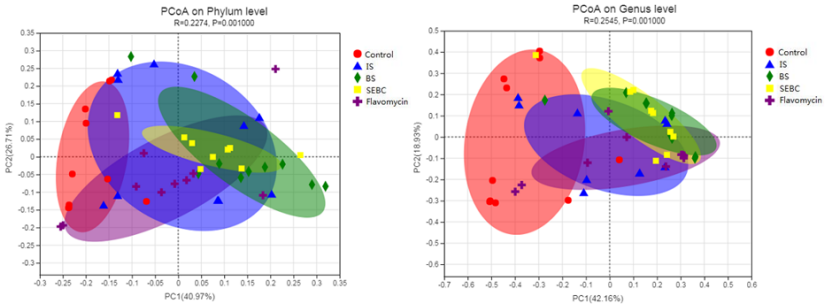

Fig 6b PCoA analysis on bacterial composition (In phylum and genus level).

Figure 6

The composition of bacteria in ileal mucous membrane. Fig. 6a The circos figure of relationship between bacterial composition (genus level). In circos figure, left half circle is the bacterial components in different treatment. Colored belts in outer layer are treatments, and colored belts in inner layer are bacterial species. The length of the belts is the proportion of bacterial abundances. The right half circle means the proportion of certain bacterial species contained in treatments. Colored belts in outer layer are bacterial species, and colored belts in inner layer are treatments. The length of the belts is the proportion of bacterial abundances. Fig. 6b PCoA analysis on bacterial composition (genus level). Fig. 6c One-way ANOVA analysis on bacterial composition (genus level). * mean significant difference at 0.05 levels (P<0.05), **mean significant difference at 0.01 levels (P<0.01), *** mean significant difference at 0.001 levels (P < 0.001).

Figure 7 Function classification based on bacterial composition.

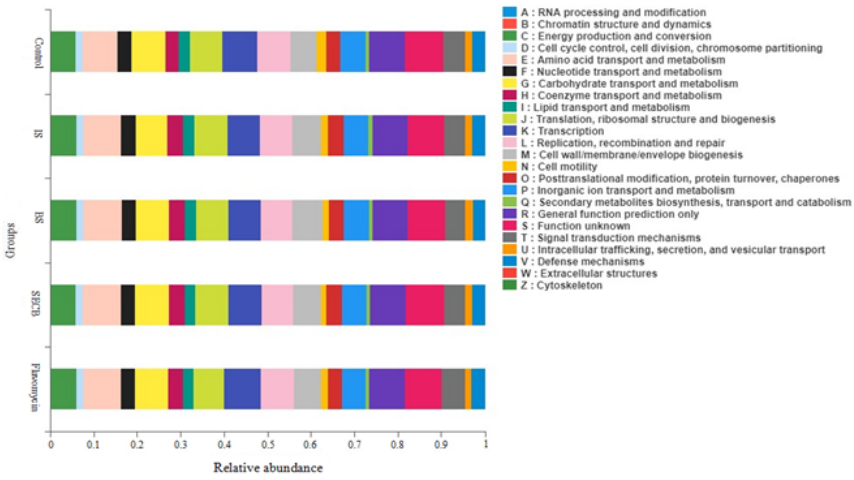

Fig. 7a KEGG pathway function classification.

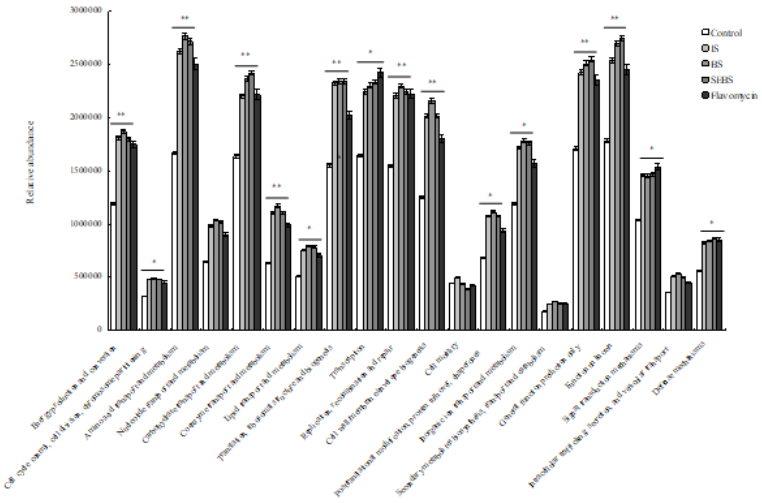

Fig. 7b One-way of ANOVA analysis between bacterial composition and function.

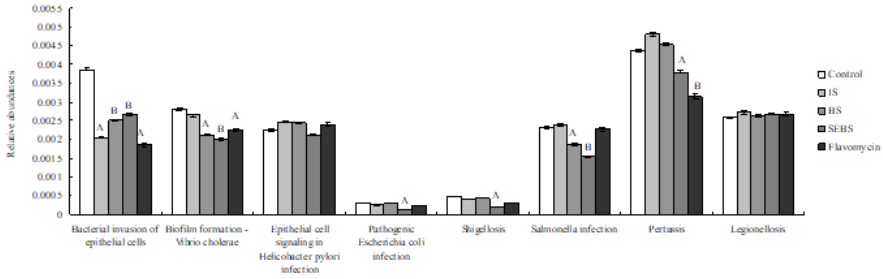

Fig. 7c The relative abundance of pathogen in One-way of ANOVA analysis of KEGG pathway function classification caused by pathogenic bacteria.

Figure 7

Function classification based on bacterial composition. Fig. 7a KEGG pathway function classification. STAMP software was applied to detect the differentially abundant Kyoto Encyclopedia of Genes and Genomes (KEGG) pathways among groups with false discovery rate correction. Fig. 7b One-way of ANOVA analysis between bacterial composition and function. * mean significant difference at 0.05 levels (P<0.05), **mean significant difference at 0.01 levels (P<0.01). Fig. 7c The relative abundance of

pathogen in One-way of ANOVA analysis of KEGG pathway function classification caused by pathogenic bacteria. The different superscript capital letters in the same color of column in the same experimental duration mean significant difference at 0.01 levels (P<0.01).

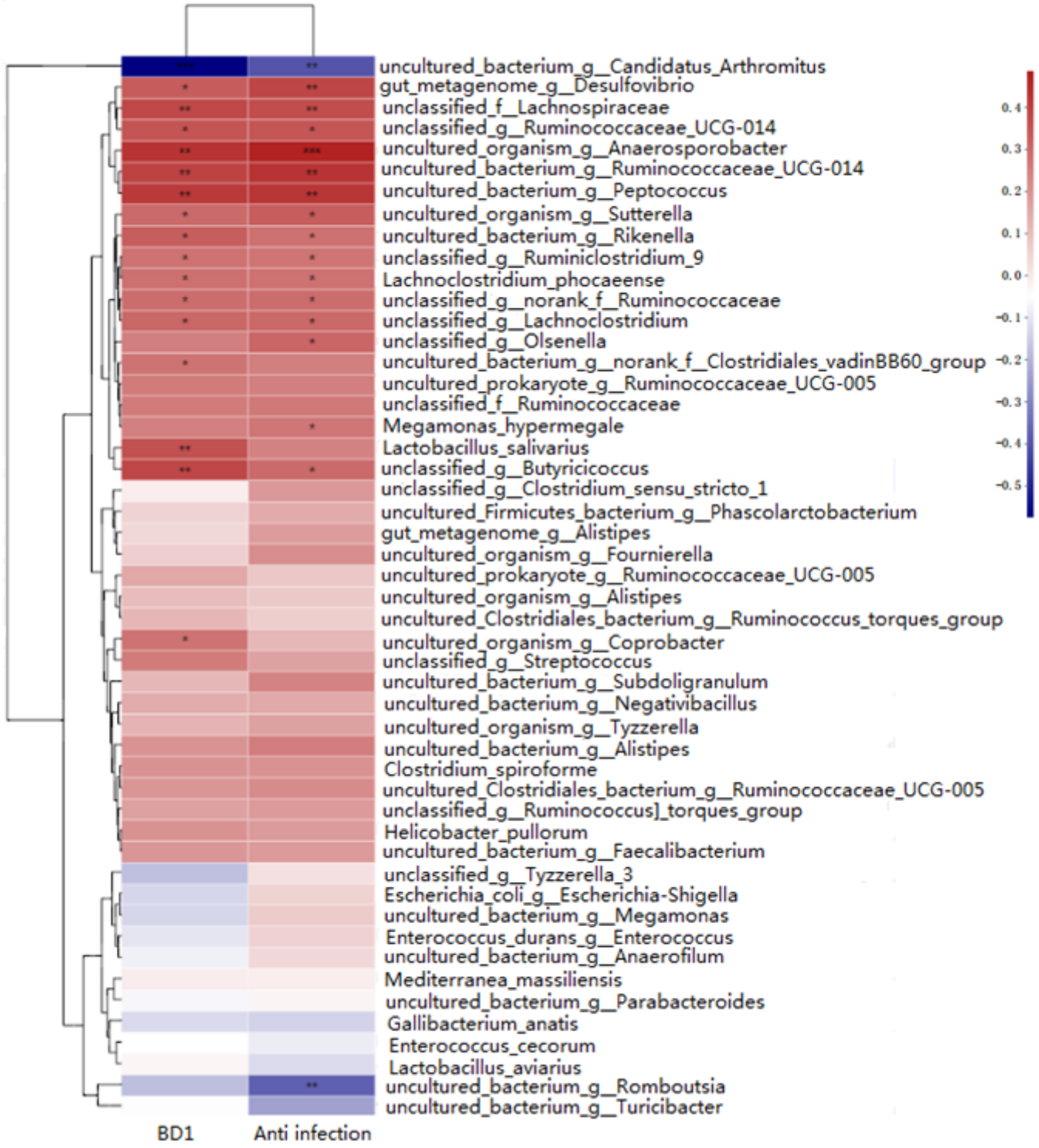

Figure 8

The Spearman's correlation analysis on bacteria and environmental factors BD1 and anti infection. * mean significant difference at 0.05 levels (P<0.05), **mean significant difference at 0.01 levels (P<0.01),

*** mean significant difference at 0.001 levels (P < 0.001).

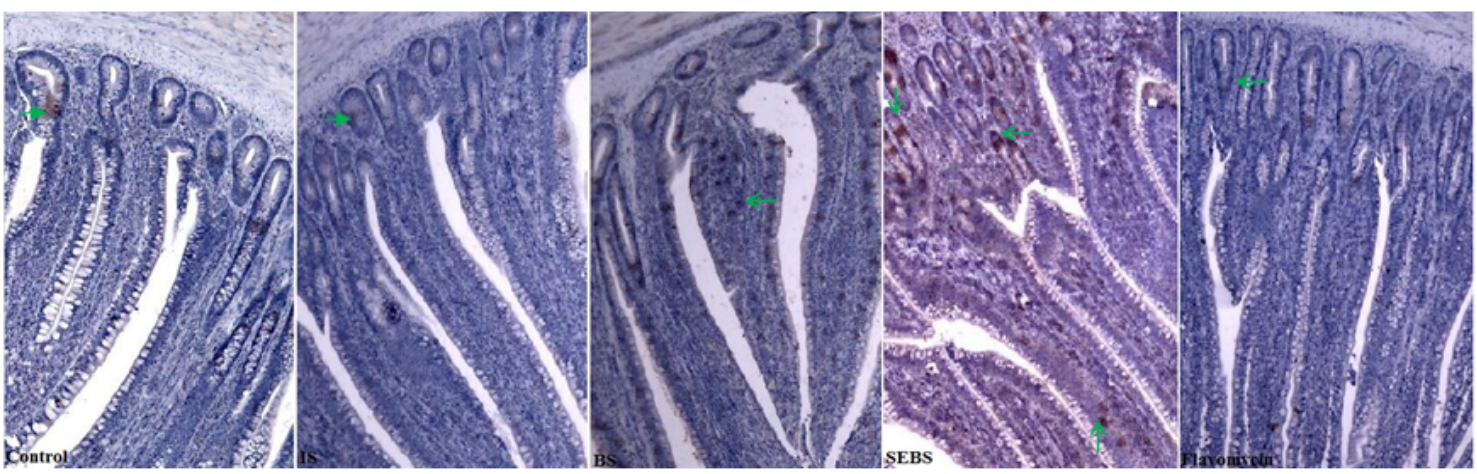

Fig. 9a Immunohistochemical of BD1 in ileal of groups S (×100 magnification).

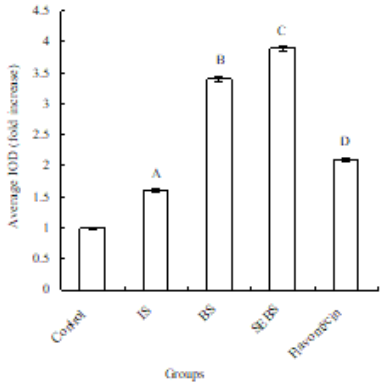

Fig. 9b Analysis of BD1 protein levels.

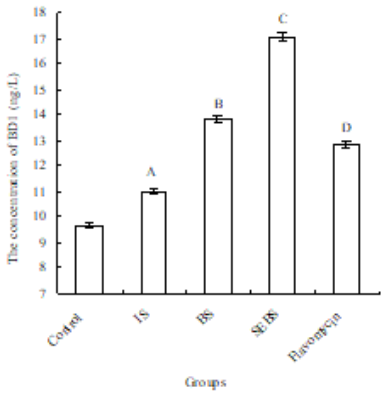

Fig. 9c The levels of BD1 (ELISA assay)

Figure 9

Development of ileal micro-structure of groups. Fig. 9a Immunohistochemical of BD1 in ileal of groups. Fig. 9b Analysis of BD1 protein levels. Fig. 9c The levels of BD1 (ELISA assay). The different superscript capital letters in the same color of column in the same experimental duration mean significant difference at 0.01 levels (P<0.01).

Figure 10 The expression of cytokines of mouse intestinal crypt cells in different treatment.

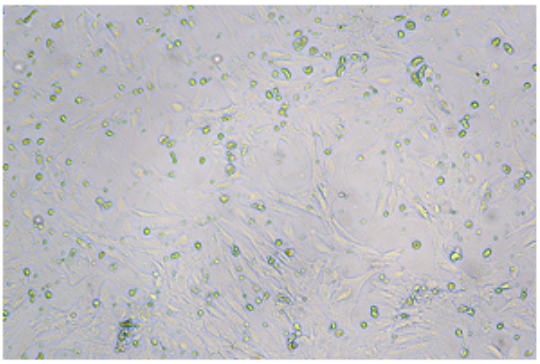

Fig. 10a Mouse intestinal crypt cells cultured for 24h, stained with 0.4% trypan blue dye (×400 magnification).

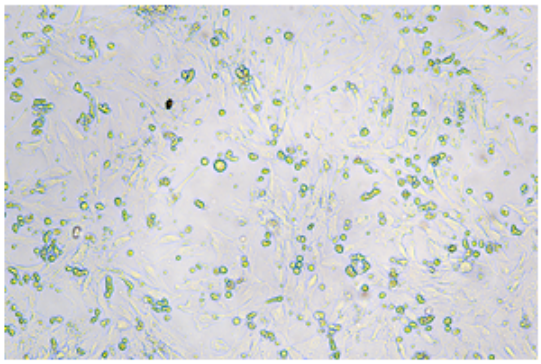

Fig. 10b Mouse intestinal crypt cells cultured for 48h, stained with 0.4% trypan blue dye(×400 magnification).

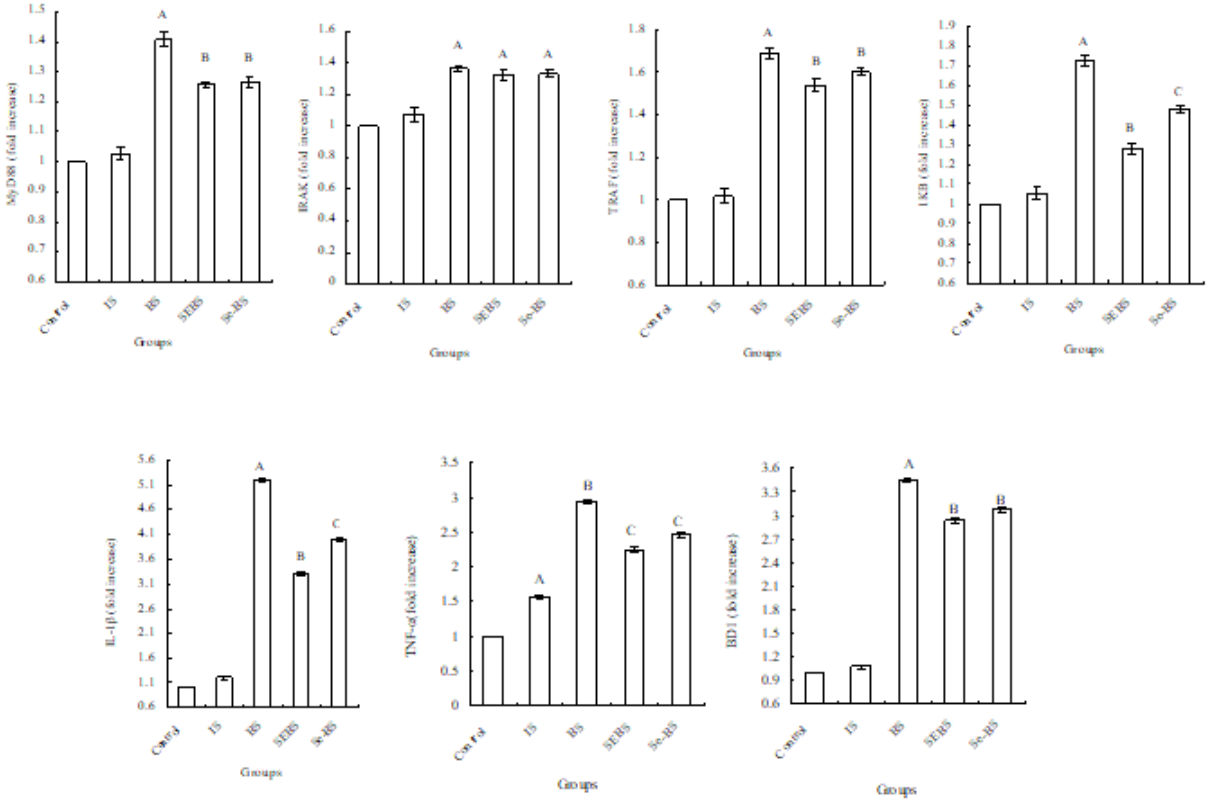

Fig. 10c The expression of cytokines crypt cells.

Figure 10

Figure 10 The expression of cytokines of mouse intestinal crypt cells in different treatment. Fig. 10a Mouse intestinal crypt cells cultured for 24h, stained with 0.4% trypan blue dye (×400 magnification). Fig. 10b Mouse intestinal crypt cells cultured for 48h, stained with 0.4% trypan blue dye(×400 magnification). Fig. 10c The expression of cytokines crypt cells. mRNA: glyceraldehyde phosphate dehydrogenase (GAPDH) internal control was used for statistical comparison. Values are means, with standard errors are

represented by vertical bars. Mean value was significantly different from that of the control group by one-way ANOVA followed by Tukey's multiple comparison tests: the different superscript capital letters in the same color of column in the same experimental duration mean significant difference at 0.01 levels (P<0.01).

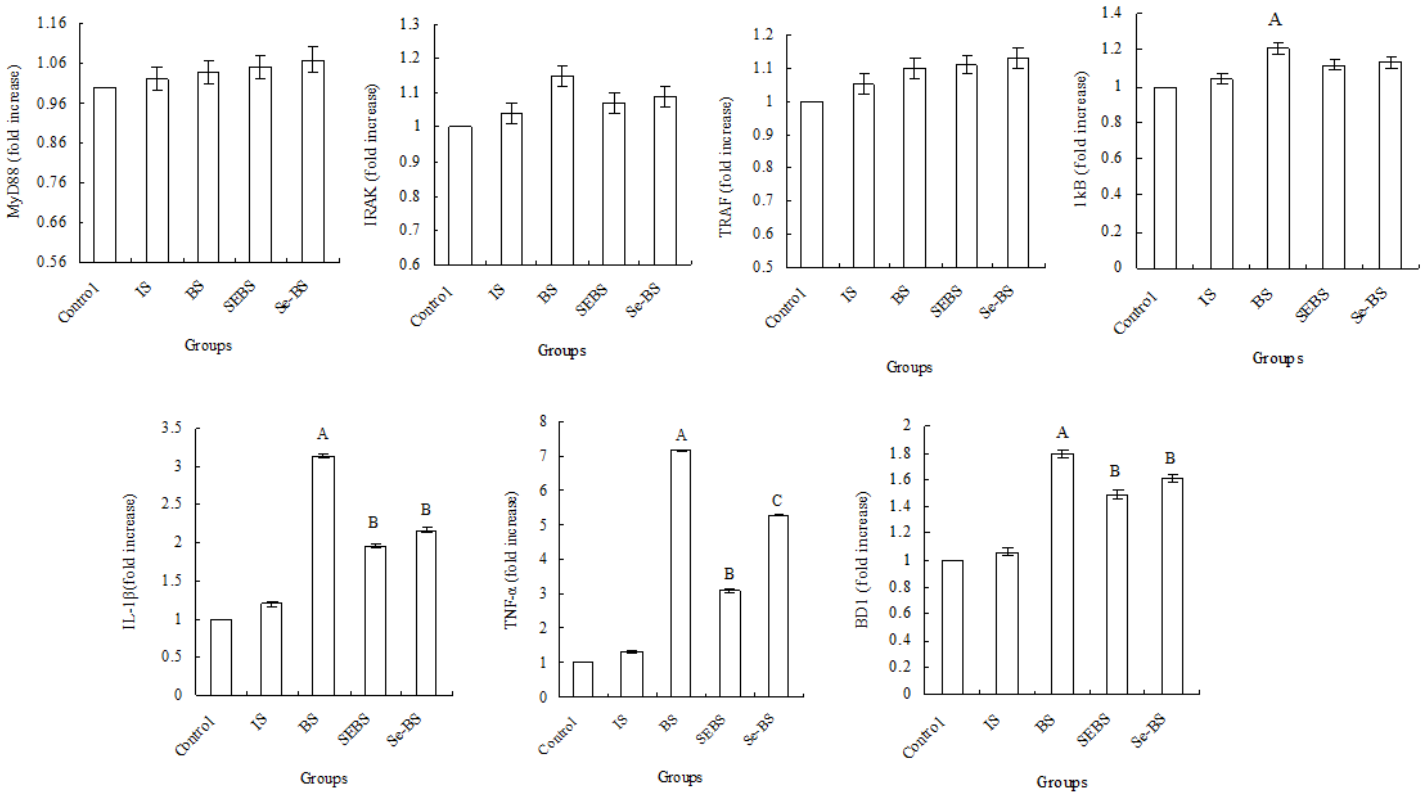

Figure 11

The expression of cytokines in crypt cells pre-treated with anti-TLR2 protein. mRNA: glyceraldehyde phosphate dehydrogenase (GAPDH) internal control was used for statistical comparison. Values are means, with standard errors are represented by vertical bars. Mean value was significantly different from that of the control group by one-way ANOVA followed by Tukey's multiple comparison tests: the different superscript capital letters in the same color of column in the same experimental duration mean significant difference at 0.01 levels (P<0.01).

Supplementary Files

This is a list of supplementary files associated with this preprint. Click to download.

- SUPPLEMENT.doc
- SUPPLEMENT.doc
- supplementarytext1differencesinspecies20200307.xls
- supplementarytext1differencesinspecies20200307.xls